2014-05

Vibrational spectroscopy for probing molecular-level interactions in organic films mimicking biointerfaces

Advances in Colloid and Interface Science, Amsterdam : Elsevier BV, v. 207, p. 199-215, May 2014
http://www.producao.usp.br/handle/BDPI/50223

Advances in Colloid and Interface Science 207 (2014) 199–215

Contents lists available at ScienceDirect

Advances in Colloid and Interface Science

journal homepage: www.elsevier.com/locate/cis

Vibrational spectroscopy for probing molecular-level interactions in organic films mimicking biointerfaces

Diogo Volpati [a], Pedro H.B. Aoki [b], Priscila Alessio [b], Felippe J. Pavinatto [a], Paulo B. Miranda [a], Carlos J.L. Constantino [b], Osvaldo N. Oliveira Jr. [a,*]

[a] São Carlos Institute of Physics, University of São Paulo, CP 369, São Carlos, SP 13560-970, Brazil
[b] Faculty of Science and Technology, UNESP, Presidente Prudente, CEP 19060-900 SP,Brazil

ARTICLE INFO

Available online 30 January 2014

Keywords:
Thin nanostructured films
Vibrational spectroscopy
Cell-membrane models
Surface functionalization
Biomolecules
Biointerfaces

ABSTRACT

Investigation into nanostructured organic films has served many purposes, including the design of functionalized surfaces that may be applied in biomedical devices and tissue engineering and for studying physiological processes depending on the interaction with cell membranes. Of particular relevance are Langmuir monolayers, Langmuir–Blodgett (LB) and layer-by-layer (LbL) films used to simulate biological interfaces. In this review, we shall focus on the use of vibrational spectroscopy methods to probe molecular-level interactions at biomimetic interfaces, with special emphasis on three surface-specific techniques, namely sum frequency generation (SFG), polarization-modulated infrared reflection absorption spectroscopy (PM-IRRAS) and surface-enhanced Raman scattering (SERS). The two types of systems selected for exemplifying the potential of the methods are the cell membrane models and the functionalized surfaces with biomolecules. Examples will be given on how SFG and PM-IRRAS can be combined to determine the effects from biomolecules on cell membrane models, which include determination of the orientation and preservation of secondary structure. Crucial information for the action of biomolecules on model membranes has also been obtained with PM-IRRAS, as is the case of chitosan removing proteins from the membrane. SERS will be shown as promising for enabling detection limits down to the single-molecule level. The strengths and limitations of these methods will also be discussed, in addition to the prospects for the near future.

Contents

1. Introduction

The importance of biointerfaces has been emphasized in view of the increasing use of biomaterials and for biomedical applications, both in diagnosis as well as in therapy. Adequate interactions at the interface are necessary between biomaterials replacing parts of living systems and living tissues [1,2]. A clear example is the area of tissue engineering [3], for cell growth and differentiation are essential for producing artificial organs [4–8] and implants [9–19]. In drug delivery systems, surface coatings may be required for some types of release [20–24]. For the design of new pharmaceutical drugs, an important ingredient is the

* Corresponding author. Tel./fax: +55 16 3373 9825.
E-mail address: chu@ifsc.usp.br (O.N. Oliveira).

0001-8686/$ – see front matter © 2014 Elsevier B.V. All rights reserved.
http://dx.doi.org/10.1016/j.cis.2014.01.014

identification of the mode of action which is normally associated with the cell membranes (i.e. biointerfaces). In clinical diagnosis, the fabrication of novel biosensors relies increasingly on functionalized surfaces that may also be considered as biointerfaces [25–29].

Biointerfaces are now investigated using a myriad of experimental methods and computer simulations [30]. These include techniques to probe surface properties such as wetting and adhesion, methods to determine structure, e.g. X-ray [31–33] and neutron reflectivity [34–37], several types of microscopy and various spectroscopic methods [38–43]. For the purposes of this review paper, we shall concentrate on the vibrational spectroscopy methods, whose use will be exemplified for two types of systems associated with biointerfaces. The first is model cell membranes that are mimicked with nanostructured films, including Langmuir monolayers [44–46], Langmuir–Blodgett (LB) films [47,48] and layer-by-layer (LbL) films [49–51]. The second type of system is functionalized surfaces where biomolecules are employed in coatings for several applications.

The review is organized as follows. Section 2 brings a brief description of the three vibrational spectroscopic methods considered here, namely infrared absorption-based spectroscopy, sum-frequency generation (SFG) spectroscopy and surface-enhanced Raman scattering (SERS) spectroscopy. Examples of their use for cell membrane models and functionalized surfaces are given in Section 3. We emphasize here that our survey of possible uses of these methods is by no means exhaustive; we simply selected a variety of papers to illustrate the strengths of the methods for biointerfaces. Section 4 is dedicated to a comparison of strengths and limitations of the methods considered, which is followed by Conclusion and future prospects in Section 5.

2. Vibrational spectroscopy techniques

In this section, a brief introduction to the spectroscopy techniques most useful for biointerfaces will be provided, with the aim of offering some background for understanding the results and contributions to be discussed throughout the review paper. Experimental details and the theoretical background behind the techniques are either omitted or presented very briefly, and the readers are referred to the literature. For instance, readers interested in the use of vibrational spectroscopy for investigating biological applications may consult ref. [52]. Because it is less frequently used, sum-frequency generation (SFG) is described at a greater length.

2.1. Infrared absorption-based spectroscopic methods

The electromagnetic radiation in the infrared (IR) region of the spectra has oscillation frequencies that match the characteristic frequency of vibrational modes of matter, and therefore IR spectroscopies have been ubiquitously used as characterization techniques. A variation of the traditional transmission Fourier Transform Infrared spectroscopy (FTIR), developed by *Greenler* [53], was based on measuring the reflected light from a film supported on reflective substrates (e.g. metals), and is now referred to as IRRAS (infrared reflection-absorption spectroscopy). With IRRAS one has improved sensitivity and orientation specificity, which is achieved with the interference of the incident and reflected components of the electric field, attained at incidence angles of ca. 80°, and the surface selection rule according to which only *p*-polarized light will be reflected from the surface [53]. Derivations of reflection–absorption IR technique were developed over the years, which include the internal total reflection–absorption FTIR spectroscopy (nowadays known as ATR — attenuated total reflection) [54]. ATR is now among the most useful tools to characterize biological films supported by solid crystals [55,56]. As a method to probe biointerfaces, IRRAS had its applicability largely expanded when it was adapted to Langmuir monolayers [57,58].

An extension to IRRAS was made by Golden and co-workers in the early 1980s [59], where the incident polarized infrared source had its beam polarization alternated between *s* and *p* at a frequency of tens of kHz. They were then able to calculate the differential reflectivity (S), given in Eq. (1), where R_p and R_s are, respectively, the reflectivities for *p* and *s* polarizations. The new variant was named PM-IRRAS, where the letters PM stand for polarization modulated.

$$S = \frac{R_p - R_s}{R_p + R_s}. \quad (1)$$

Blaudez and co-workers [60,61] realized the importance of PM-IRRAS and applied it to the characterization of Langmuir films. Water is not a perfect reflector and therefore both *p* and *s* polarizations can be simultaneously absorbed because the surface selection rule is not applicable for the air/water interface. Since *p*-polarized light is more sensitive to vertically oriented dipoles and *s*-polarized beam is sensitive to horizontally oriented ones, the relative orientation of chemical groups from the film constituents can be estimated from the analysis of the differential reflectivity. Moreover, by subtracting the bare water reference spectrum from the film reflectivity ($\Delta S = S_{film\ +\ water} - S_{water}$), contributions to the signal can be filtered out from isotropically oriented molecules, such as CO_2 and H_2O (the latter from vapor right above the film or from the subphase beneath it), which are the main noise sources to the final spectrum.

In the 1980s another FTIR-related technique was developed based on the enhancement of IR absorption by *plasmons* in metallic nanostructures, which was named Surface-enhanced infrared-absorption spectroscopy (SEIRA). In recent years, SEIRA has been used to probe metal-supporting biological and organic thin films [62,63].

Because of the large number of contributions in the literature associated with IR-related methods, we chose a few examples of the use of ATR, SEIRA, IRRAS and PM-IRRAS to characterize films mimicking biointerfaces to be mentioned in this review, while many others can be found in other pieces in the literature [64,65].

2.2. Sum-Frequency Generation spectroscopy

Sum-Frequency Generation spectroscopy (SFG) is a nonlinear optical spectroscopic technique with which to obtain the vibrational spectrum of interfacial molecules, discriminating them from those in the bulk material. It is therefore surface-specific, with intrinsic selectivity to interfacial contributions. Here we describe only the fundamentals of SFG spectroscopy. A detailed theory can be found elsewhere [66–68], and references [69,70] are tutorial reviews of its applications to many fields of surface science. Recent reviews of applications of SFG spectroscopy to selected fields are also available [71–73].

In SFG spectroscopy, two high-intensity laser beams at frequencies ω_{vis} and ω_{IR} overlap at an interface and generate an output beam at frequency $\omega_{SFG} = \omega_{vis} + \omega_{IR}$ in the reflection direction. The intensity of the SFG signal is proportional to the square of the effective second-order nonlinear susceptibility of the interface, $\chi^{(2)}_{eff}(\omega_{SFG} = \omega_{vis} + \omega_{IR})$. As second-order process, SFG is forbidden in media with inversion symmetry, such as gases, bulk liquids, amorphous solids and most crystals of achiral molecules, but allowed at interfaces where the inversion symmetry is broken. This is why SFG spectroscopy is intrinsically sensitive to interfaces. Since the process relies on broken inversion symmetry, only molecules without inversion symmetry may be detected in SFG. However, if such molecules arrange at an interface with random orientations, the net SFG signal vanishes. Conversely, if there is a substantial SFG signal, it can be concluded that molecules have a net average orientation at the interface. Thus, we can obtain information about the average orientational ordering of the interfacial molecules. For vibrational spectroscopy, ω_{IR} is tunable in the mid-infrared, (in the range of the vibrational modes of the surface molecules), while ω_{vis} is a fixed frequency within the visible spectrum, so that ω_{SFG} is also in the visible–UV and can be detected with high sensitivity. In some cases, ω_{vis} may be tunable as well, yielding the electronic spectrum of interfacial

molecules [74], although this is less common due to the added complexity in the experimental setup and data analysis.

For the analysis of the vibrational spectrum, the intensity of the SFG signal may be expressed as

$$I_{SFG} \propto \left|\chi^{(2)}_{eff}\right|^2 = \left|\chi^{(2)}_{NR} + \chi^{(2)}_{R}\right|^2 = \left|\chi^{(2)}_{NR} + N_s \sum_q \frac{A_q}{\omega_{IR} - \omega_q + i\Gamma_q}\right|^2 \quad (2)$$

where $\chi^{(2)}_{NR}$, $\chi^{(2)}_{R}$, N_s, A_q, ω_q, Γ_q are the nonresonant and resonant contributions to $\chi^{(2)}_{eff}$, the surface density of molecules and the oscillator strength, resonant frequency and linewidth of the q-th vibrational mode, respectively. From Eq. (2) one notes that when ω_{IR} is near the frequency of molecular vibrations, the SFG output is resonantly enhanced, yielding a vibrational spectrum of the interface. Eq. (2) also demonstrates a feature of nonlinear spectroscopic methods that are very different from their linear counterparts: there is *interference* of the resonant contribution, $\chi^{(2)}_{R}$, with the non-resonant background, $\chi^{(2)}_{NR}$, leading to changes in the spectral lineshape which depend on both the magnitude and phase of $\chi^{(2)}_{NR}$, and also on the presence of nearby resonances. Therefore, a quantitative analysis of SFG spectra requires curve fitting to Eq. (2) in order to obtain the amplitudes, frequencies and linewidths of the resonances. In particular, the peak SFG intensity only occurs at the resonance ($\omega_{IR} = \omega_q$) and is proportional to the square of the mode amplitude A_q if the nonresonant background is negligible. Furthermore, if a mode is broadened but keeps the same amplitude A_q, the area under the peak is *not* constant, as it would be in conventional IR or Raman spectroscopy.

As in any vibrational spectroscopy, information on the molecular arrangement at the interface is obtained indirectly by the interpretation of SFG spectra. For instance, the frequency/linewidth of vibrational resonances could be related to the interaction of molecular moieties with neighboring molecules, such as in the case of H-bonding. Besides the spectral information, it is possible to obtain qualitative, and sometimes quantitative [75] information on the molecular orientation at the interface within the following framework. Since the surface nonlinear susceptibility is a third-rank tensor, $\chi^{(2)}_{ijk}$, the measured effective susceptibility $\chi^{(2)}_{eff}$ depends on the polarizations (*s* or *p*) of the input and output beams. For an isotropic sample along the surface (*xy* plane) and with ω_{SFG} and ω_{vis} away from electronic resonances, the only nonvanishing $\chi^{(2)}$ elements are $\chi^{(2)}_{zzz}$, $\chi^{(2)}_{xxz} = \chi^{(2)}_{yyz}$, and $\chi^{(2)}_{zxx} = \chi^{(2)}_{zyy} = \chi^{(2)}_{xzx} = \chi^{(2)}_{yzy}$, which can be probed, respectively, with the polarization combinations *ppp*, *ssp*. and *sps* (from the first to last, the letters indicate the polarization of the SFG, visible and mid-IR beams). For each vibrational mode, these tensor elements are related to the molecular second-order polarizability by a transformation of coordinates from the molecular frame (ξ,η,ζ) to the laboratory frame (x, y, z),

$$\chi^{(2)}_{ijk} = N_s \sum_{\xi\eta\zeta} \left\langle \left(\hat{i}\cdot\hat{\xi}\right)\left(\hat{j}\cdot\hat{\eta}\right)\left(\hat{k}\cdot\hat{\xi}\right)\right\rangle \alpha^{(2)}_{\xi\eta\zeta} \quad (3)$$

where the angular brackets indicate an average over the molecular orientational distribution. Since $\alpha^{(2)}_{\xi\eta\zeta}$ is proportional to both the IR dipole moment and Raman polarizability derivatives with respect to the normal coordinate, $\frac{\partial \mu_\xi}{\partial Q}$ and $\frac{\partial \alpha_{\xi\eta}}{\partial Q}$, respectively, it is usually possible to obtain the ratio of the nonvanishing $\alpha^{(2)}_{\xi\eta\zeta}$ tensor elements. Therefore, for a known $\alpha^{(2)}_{\xi\eta\zeta}$ and with the measured $\chi^{(2)}_{ijk}$ the orientation of the moiety responsible for that vibration may be obtained. Eq. (3) also highlights another interesting feature of SFG spectroscopy: if the molecular orientation inverts from upward to downward ($z \rightarrow -z$) the sign of $\chi^{(2)}_{R}$ changes. The interference with $\chi^{(2)}_{NR}$, from the sample or introduced externally in a heterodyne detection scheme [71], reveals this sign change, which can be used to determine the absolute orientation of the asymmetric molecules (up or down).

One particularly interesting aspect of SFG spectroscopy with regard to the biomimetic systems considered in this review is the ability to probe (at least qualitatively) the conformation of alkyl chains, a major component of all lipids and other biomolecules. As shown by *Guyot-Sionnest* et al. [76], if a Langmuir monolayer is compressed to a highly condensed phase, where the alkyl chains are known to be in the *all-trans* conformation and nearly vertical, the SFG spectrum in the CH stretch range is dominated by the terminal methyl group, even though there is usually an overwhelmingly large number of methylene groups along the alkyl chain. This is due to the inversion symmetry of the in-plane arrangement of CH_2 groups, which point in opposite directions (and perpendicular to the chain axis), leading to a cancelation of their contribution. On the other hand, the CH_3 groups are well ordered, pointing away from the subphase and giving a strong contribution to the SFG spectrum. As the monolayer is expanded, thermally activated *gauche* conformations appear, breaking the symmetry of the CH_2 arrangement and making the CH_3 more widely distributed. This leads to an increase of the methylene and a reduction of the methyl symmetric stretches. Therefore, the ratio of their amplitudes can be used to quantify the relative conformational order of lipid chains [77,78].

One question that always arises is how deep into the interface is SFG spectroscopy probing. Since the technique relies on breaking the inversion symmetry, the answer depends on the particular system investigated. For instance, it could be just a monolayer, as in the case of lipids in a Langmuir film or for the surface of a surfactant solution, where the adsorbed monolayer is oriented with chains away from the liquid, but the molecules in solution have random orientations. However, for charged interfaces in contact with an electrolyte, the electrical field within the electrical double layer breaks the inversion symmetry near the interface, and the whole depth of the double layer (typically up to tens of nm) may contribute to the spectrum. This has been clearly demonstrated in the case of the OH stretches of interfacial water [79]. Finally, for a solution of chiral molecules there is no inversion symmetry, since inversion would change the handedness of the molecules. In this case, the SFG signal may be generated from the bulk solution, up to the coherence length for the particular experimental configuration — usually several hundred nm, for the reflection geometry [80].

For the implementation of SFG spectroscopy, usually ultrashort pulsed laser systems are used (from 100 fs to tens of ps) to attain the high peak intensities at the sample, but with low repetition rates (tens of Hz to a few kHz) to avoid average heating and damage to the samples (typical average powers of a few mW only). The most popular laser systems used to date can be divided in two categories: (i) ps pulse duration and low repetition rate (~10 Hz), where the SFG spectrum is obtained by scanning the frequency of the mid-IR pulse generated by an optical parametric amplifier (OPA) and measuring the intensity of the SFG signal, and (ii) ~100 fs pulse duration and higher repetition rates (~1 kHz), where the bandwidth of the mid-IR pulse produced by the OPA is large enough to allow measuring the whole SFG spectrum at once by mixing the mid-IR pulse with a ps visible pulse and detecting the SFG signal on a multichannel spectrometer. These latter systems have the advantage that laser intensity fluctuations do not affect the quality of the SFG spectra, generally yielding higher signal-to-noise data.

2.3. Surface Enhanced Raman Scattering (SERS)

The vibrational spectroscopic technique based on the Raman scattering, i. e., the inelastic scattering of light, has limited use for low concentrated systems such as diluted solutions, ultrathin films and interfaces due to the small cross section (10^{-30} cm^2/molecule). Making use of the SERS effect is thus a viable alternative owing to signal enhancement by several orders of magnitude when the target molecule is placed close to metallic nanoparticles. The average enhancement factor ranges from 10^3 to 10^6, and can reach up to 10^{10}at the interstices of metallic nanoparticles, referred to as hot spots [81,82]. The enhancement of the Raman signal can be explained according to two main mechanisms of different origins: the electromagnetic effect and the chemical effect (or charge transfer).

In the electromagnetic effect, SERS arises from amplification of the electric field (E) of the incident radiation surrounding the surface of metallic nanoparticles. The latter can sustain localized surface plasmon resonances (LSPR), which leads to an amplification factor proportional to E^4 [81,82]. The polarizability of the target molecule is not affected, i.e., this effect is independent of the chemical nature and type of metal–molecule interaction (physisorption). It depends on the dielectric function of the metal and of the surrounding medium, the size, shape and aggregation of the metallic nanoparticles. Because incident radiation from lasers is normally in the visible, noble metals such as Au, Ag and Cu, exhibit suitable dielectric functions. A simplified explanation for a spherical isolated metallic nanoparticle can be found in [83]. On the other hand, amplification based on the chemical effect results from the interaction between the metal and the target molecule adsorbed on sites where there is strong electron–photon coupling. Changes in molecular polarizability generated by the interaction between the molecule and the surface (chemisorption) are now relevant. The latter can lead to signal enhancement factors up to 10^2. Both electromagnetic and chemical mechanisms may contribute simultaneously to the Raman signal [81].

Gold (Au), silver (Ag) and copper (Cu) nanoparticles (NPs) are used as SERS active surfaces, especially the ones close to the spherical shape. A variety of nanoparticles with different shapes, including nanorods [84], nanoprisms [85,86], and nanocubes [86] have also been developed. *Li* et al. [87] proposed an approach for obtaining SERS based on shell-isolated nanoparticles (SHIN). The key factor was the ultrathin shell of SiO_2, which prevents the nanoparticles from aggregating and separates them from direct contact with the probed material. Another advantage is the possibility of achieving surface-enhanced fluorescence (SEF), since the silica shell avoids fluorescence quenching by metal nanoparticles, as shown by *Guerrero* et al. [88].

SERS has been competitive in the investigation of biological systems, for targets can be detected without the need of labels. Unlike fluorescence, SERS provides information about the molecular structure and chemical composition of the sample. Besides, SERS enhancement factor enables detection limits comparable to fluorescence spectroscopy, down to the single-molecule level. Short acquisition times and low laser powers can often be used for SERS as a result of the signal enhancement [89], which is also favorable for biological samples [90].

3. Understanding biological interfaces with spectroscopy methods

The term “biological interfaces” may refer to systems involving external bodies that interact with living tissues, as in biomedical implantable devices or surgery tools in action, and even interfaces of two inanimate biomaterials in a biological context, e.g. titanium knobs and epoxy resins in dental prosthetics. But the environment better described by this term is the one in which cells and/or tissues interact with themselves. Ultimately, such systems interface through cell membranes interactions involving major membrane components such as phospholipids, cholesterol and proteins. Hence, nanostructured films made from these molecules are suitable for models to mimic the interfaces.

The concept of using nature's inspired nanoscale self-assembly to build bottom-up structures that mimic biological architectures is already well diffused in laboratories and industry worldwide [91]. The most employed films and assemblies are Langmuir and Langmuir–Blodgett (LB) films, layer-by-layer (LbL) films and liposomes or vesicles [92]. They are used to model cell membranes [93], tissue engineering and cell adhesion interfaces [94]. Also worth mentioning is that nanotechnology has impacted the study of biological interfaces with fabrication of artificial biointerfaces using lithography techniques [95].

3.1. Cell membrane models

The main aim in using Langmuir monolayers as cell membrane models [96,97] is to understand how molecules of biological interest interact with the membrane. This is important for various reasons, including the identification of the mode of action of pharmaceutical drugs [98,99] and the attempts to understand toxicological properties of nanoparticles [100], to name just a few. Important features investigated in this type of work are whether the molecules penetrate into the membrane, how they affect the membrane elasticity and whether concentration effects from the guest molecules exist. Traditional methods to characterize Langmuir monolayers, such as surface pressure and surface potential measurements and microscopy techniques, may give valuable information on the possible penetration of the guest molecules and on the changes in elasticity. However, in order to be sure that the guest molecules indeed penetrate into the monolayer and to establish the chemical groups involved in the intermolecular interactions, spectroscopic techniques are necessary.

Vibrational spectroscopy methods, in particular, may provide information not only on the functional groups involved in molecular interactions but also on their orientation, and whether they are affected by hydration or H-bonding. Indeed, the importance of spectroscopy techniques for cell membrane models has already been widely acknowledged [101]. For biomolecules, perhaps the most interesting feature in PM-IRRAS studies is the possibility of verifying whether the proteins preserve their native structure, or undergo interface mediated conformational changes. This is normally done by monitoring the amide bands, which are known to be shifted when changes in the protein secondary structure occur.

The molecular structuring, orientation and hydration levels of Langmuir monolayers can be monitored with SFG, as was demonstrated for the first time decades ago [76]. Furthermore, SFG spectroscopy is unique in its ability to probe the organization of water molecules at interfaces [102], and in particular its interaction with Langmuir films [78]. Fig. 1 shows schematic diagrams depicting a liquid-expanded to liquid-condensed phase transition in a Langmuir monolayer of deuterated dipalmitoylphosphatidylcholine (DPPC-d62), where the squeezing out of water molecules around the polar headgroups upon compression could be monitored [103].

An example of how FT-IRRAS can be used to determine the orientation of biomolecules at the air–water interface was provided by *Sarangi* et al. [104] who studied interactions of L-tryptophan with DPPC. Fig. 2a shows the details of the polarized FT-IRRAS instrumentation to determine the molecular orientations for a neat monolayer of DPPC as well as the molecular orientations when the monolayer interacts with L-tryptophan. The angle of incident φ_i was varied from 25 up to 65° from the surface normal, and spectra collected for both *s* and *p* polarizations. An example is given in Fig. 2b of how the reflectance–absorbance of the CH_2 antisymmetric stretching band changes as a function of the angle of incidence φ_i and of the electric field polarization. With such a setup, one is able determine the reorientations of the DPPC polar head groups and their dependence on subphase compositions and temperature.

While penetration of guest molecules into the cell membrane model represented by Langmuir monolayers can be inferred from surface pressure isotherms, the interpretation is never unequivocal since other types of interaction may lead to expansion in the isotherms. With spectroscopic methods, on the other hand, the possible penetration can be tested beyond doubt, and for biomolecules one may even determine whether the native conformation was kept. For water-soluble proteins, in particular, several issues may be investigated. Perhaps the first is whether these proteins will adsorb onto the monolayer and under which conditions. For instance, *Diederich* et al. [105] used FTIR to show that the S-layer protein from *Bacillus sphaericus* CCM2177 does not interpenetrate but rather couples to the monolayer via lipid head groups. *Polverine* et al. [106] showed with FTIR measurements that a myelin basic protein (MBP) binds to negatively charged phospholipids thus forming a complex.

Insertion of a protein into a monolayer may change its orientation, as it occurred for the farnesylated and hexadecylated N-Ras protein, or

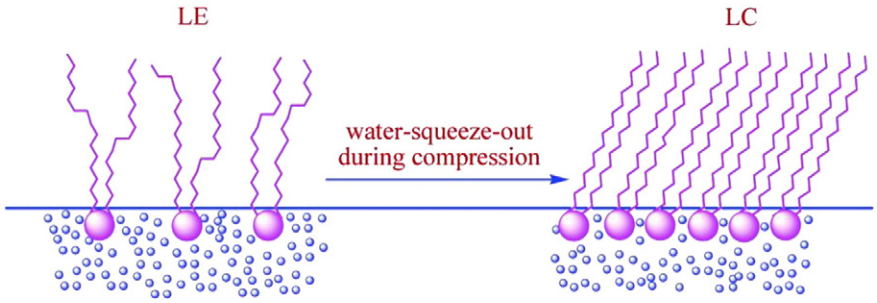

Fig. 1. Phase transitions from liquid-expanded to liquid-condensed of a Langmuir monolayer of DPPC-d26 as the barriers compressed the monolayer. The water molecules represented by blue dots are squeezed out of the head groups thus inducing the molecular ordering inferred by SFG. *Reprinted adapted with permission from* [103]. *Copyright 2014 American Chemical Society*.

simply HFar-N-Ras protein [107]. The monolayer mimicking the cell membrane was made with a mixture of POPC, brain sphingomyelin and cholesterol. Changes in orientation of the protein secondary structure were determined upon comparing experimental and simulated angle-dependent IRRAS spectra of HFar-N-Ras. The results in the reference above illustrate how modulation of polarization makes PM-IRRAS advantageous over IRRAS, since laborious angle-dependent measurements are not needed to extrapolate relative protein orientation in PM-IRRAS. There are cases in which protein adsorption leads to multilayers below a phospholipid monolayer. PM-IRRAS was employed to monitor adsorption of γ- and ω-gliadin proteins on DMPC and DMPG monolayers [108], thus forming micrometer-sized domains. The spectroscopic technique was used in conjunction with other physicochemical characterization methods to determine that γ-gliadins adsorbed under the phospholipid monolayer with β-turns and small α-helices forming multilayers, while ω-gliadins aggregates displayed a constant thickness consistent with a monolayer.

As already mentioned, one of the most important features in protein adsorption that can be interrogated with spectroscopic techniques is the preservation and the state of secondary structure. This is normally done in PM-IRRAS and SFG by observing the amide bands, which are known to be shifted to higher wavenumbers when the structure changes from β-sheet to α-helices. *VandenAkker* et al. [109] reported changes in secondary structure of amyloid fibrils by following the changes in the amide I band in SFG measurements. Fig. 3a shows the normalized SFG spectra for amide I in amyloid fibrils formed at concentrations between 3.0 and 7.5%, while Fig. 3b shows the fraction of the integrated intensity of peaks fitted to the SFG data for these two bands resulting in different proportions of β-sheet and random/α-helical structures.

The kinetics of conformational changes of proteins was studied with SFG by using an intrinsically disordered protein that is known to misfold into the β-sheet structure upon interaction with membranes [42]. Changes in the amide I band of human islet amyloid polypeptide in the air/water interface were observed after addition of dipalmitoylphosphoglycerol (DPPG), with the initial α-helical structure gradually folding into β-sheets. The same trend of secondary structure transformations was seen by *Lopes* et al. using IRRAS [110]. It is important to highlight that probing the amide I band with SFG leads to spectra free from problems associated with the background from the water OH bending mode, which is a limitation in IRRAS or PM-IRRAS.

The confirmation of preserved secondary structure was crucial in a study with septin proteins involved in the formation of amyloid-like fibers found in patients with Alzheimer's disease. *Damalio* et al. [111] studied the interaction of SEPT2 protein with DPPC and the lipid PtdIns(4,5)P2 using PM-IRRAS spectroscopy to monitor the amide I and amide II bands. The native structure of SEPT2 was preserved when it interacted with PtdIns(4,5)P2, but changes from α-helices into β-sheets were observed upon interaction with DPPC, probably because the protein was forced to expose its hydrophobic portion. The differences in behavior are probably due to the larger headgroup of PtdIns(4,5)P2 which maintains the protein hydrated at the water interface, rather than inserted in the hydrophobic tails. Furthermore, fibrils of deliberately prepared SEPT2 aggregates were unable to adsorb onto Langmuir monolayers of either DPPC or PtdIns(4,5)P2, thus indicating the irreversibility of the aggregation process.

The effects from the polysaccharide chitosan on the adsorption of proteins onto phospholipid monolayers, and its action on their possible removal from the biointerfaces, have been investigated with PM-IRRAS. The main objective was to test hypotheses associated with the action of chitosan in biological applications. Chitosan has proven antimicrobial and antifungal activities [112], and is believed to be effective for reducing cholesterol and fat [113]. Also, chitosan was shown to successfully

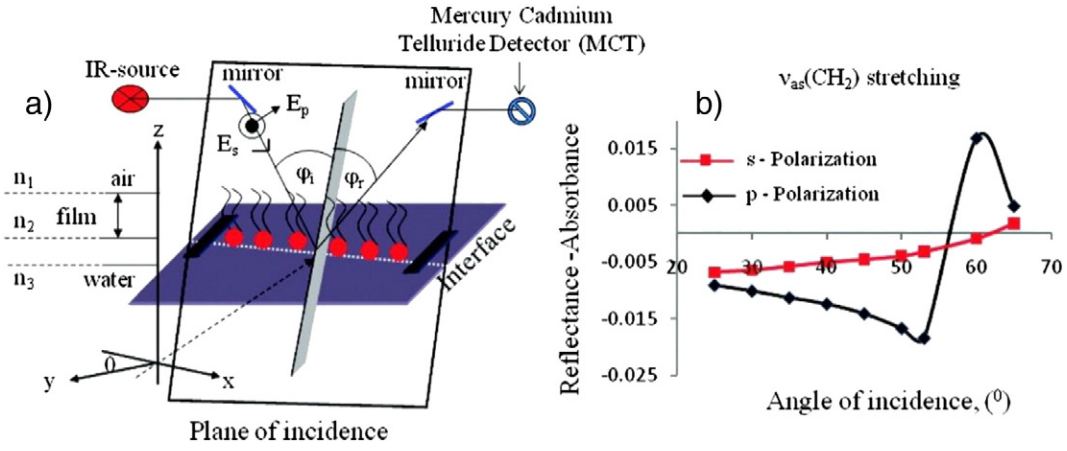

Fig. 2. (a) Configuration of modulated polarization FT-IRRAS equipment used to study the molecular orientations of a neat DPPC monolayer or when the monolayer is interacting with L-tryptophan. (b) Reflection–absorption of the monolayers depending on the light polarization and angle of incidence (Brewster angle concept). *Reprinted adapted with permission from* [104]. *Copyright 2014 American Chemical Society*.

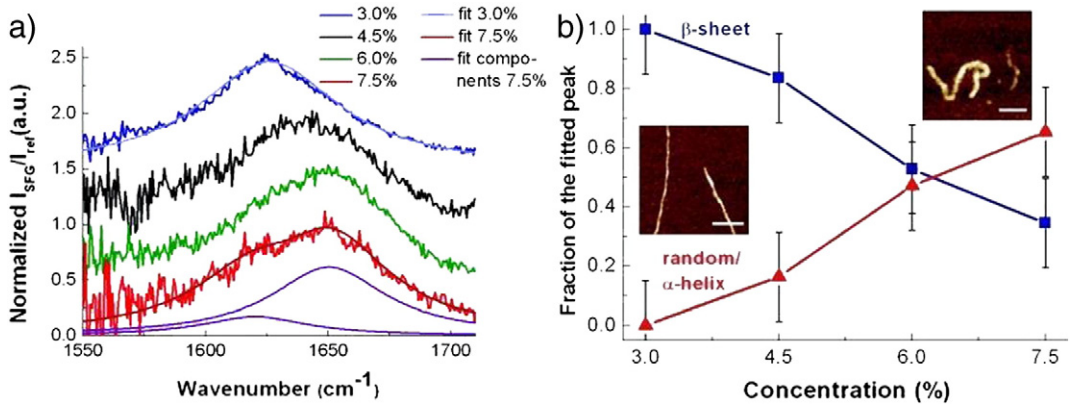

Fig. 3. (a) SFG spectra of the amyloid fibrils in the amide I spectral region at concentrations between 3.0 and 7.5%. (b) The relative presence of β-sheets and random/α-helical structures as a function of the concentration inferred by integrating the intensity of peaks fitted. The AFM images show the structure of the proteins reached by varying the concentration (Scale bar is 100 nm). *Reprinted adapted with permission from* [109]. *Copyright 2014 American Chemical Society.*

remove the protein β-lactoglobulin from whey [114], pointing to its important industrial applicability as an antiallergenic material.

Using Langmuir monolayers as biomembrane models, chitosan was found capable of removing some proteins, namely β-lactoglobulin [115] and mucin [116], from negatively charged phospholipid monolayers, for which irrefutable proof came from a comparison of PM-IRRAS spectra for the protein-containing phospholipid monolayers in the presence and absence of chitosan. Fig. 4a shows that the amide I and amide II bands from β-lactoglobulin are increasingly vanishing as time progresses with chitosan present in the subphase (Fig. 4b). A cartoon picture of the removal is shown in Fig. 5. Also relevant is the specificity of the removal action, since it only occurred when there was electrostatic attraction between the positively charged groups from chitosan and the negatively charged phospholipid, such as dipalmitoylphosphatidyl glycerol (DPPG) and dimyristoylphosphatidic acid (DMPA). The removal action did not take place in a biomembrane formed by the zwitterionic dipalmitoylphosphatidyl choline (DPPC), or for the enzymes horseradish peroxidase and urease [115].

Other effects from chitosan on membrane models made up with phospholipids and/or cholesterol were studied by *Pavinatto* et al. [77] using SFG and PM-IRRAS. While chitosan caused chain ordering in DMPA monolayers at a biomembrane-like packing state, cholesterol caused disordering, which is contradictory to its well-known role as a stiffener of the cell membrane [117,118]. This discrepancy was due to a change in the phospholipids headgroup ionization state, which was sensed as a shift to lower frequencies of the DMPA phosphate bands in PM-IRRAS spectra, in agreement with NMR data for similar lipids [119]. Furthermore, the expansion effect caused by cholesterol reflected also in the disappearance of the PM-IRRAS band at 2889 cm^{-1}, and in the decrease of an order parameter calculated from the symmetric stretching bands for CH_3 and CH_2 groups in SFG. When both materials act together the overall effect over DMPA films was an expansion. The cholesterol effect was suppressed by the stronger electrostatic-driven chitosan effect. Nevertheless, cholesterol was important for mediating chitosan penetration in the films.

As demonstrated in the results from the removal of proteins by chitosan above, the charge of the phospholipids used to mimic the cell membrane may have an important effect. *Chièze* et al. [120] studied the interaction with a protein (apolipoprotein A–I) by evaluating the influence of the charge and chain organization of the phospholipids through PM-IRRAS. Protein insertion into the phospholipid monolayer was mainly controlled by compressibility and a minimum distance between the phospholipid headgroups was required for the insertion to occur. Larger insertion was observed for phospholipids with anionic headgroups.

The mediation of another polysaccharide (ι-carrageenan) was relevant for the binding of the enzyme alkaline phosphatase from *Neurosporacrassa* (NCAP) to the synthetic phospholipid DHP (sodium salt of dihexadecylphosphoric acid) [121]. With SFG used to monitor lipid conformation and carrageenan adsorption, Zn^{+2} ions were found to mediate the interaction between DHP and the anionic polysaccharide, which adsorbed with sulfate groups orientated towards the DHP monolayer, while the hydroxyl and ether groups were exposed to the subphase. This particular conformation of the polysaccharide interacted with the protein and induced its adsorption.

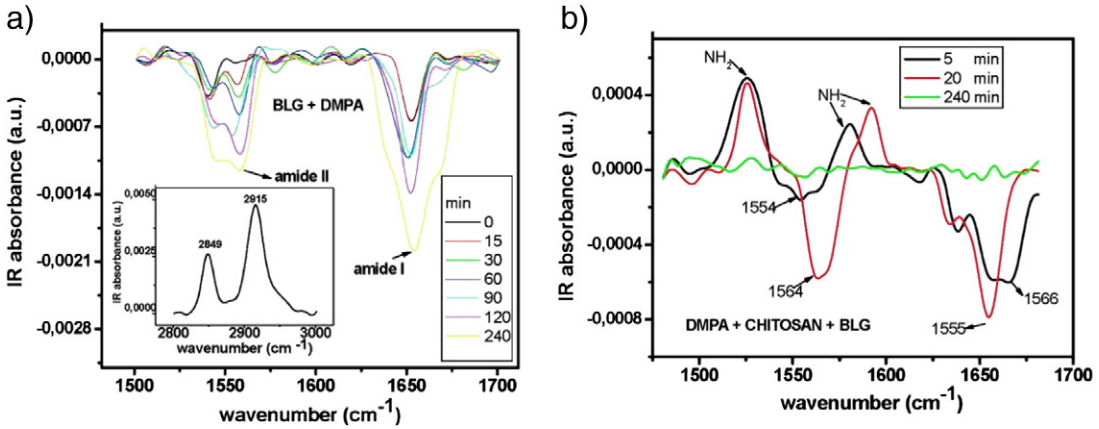

Fig. 4. (a) PM-IRRAS spectra in the range of amides I and II bands of β-lactoglobulin adsorbing on DMPA up to 240 min. (b) Adsorption is increasingly vanished when chitosan is present in the subphase, as can be seen after 240 min (green spectrum). *Reprinted adapted with permission from* [115]. *Copyright 2014 American Chemical Society.*

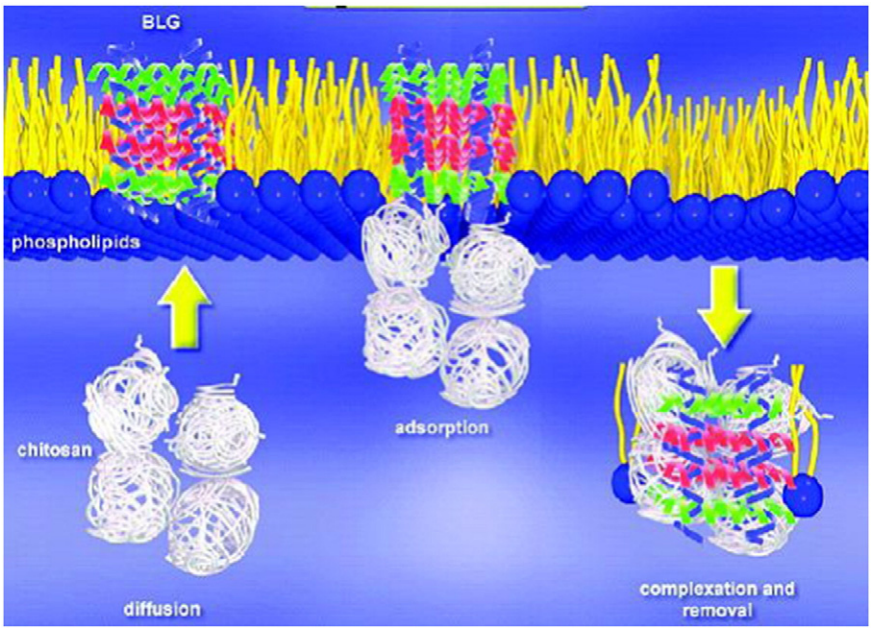

Fig. 5. Proposed model for chitosan action removing BLG from a monolayer of phospholipids. *Reprinted adapted with permission from* [115]. *Copyright 2014 American Chemical Society*.

With regard to probing the orientation of α-helical peptides, SFG and ATR-FTIR may be combined to determine peptide orientation in substrate-supported lipid bilayers by following amide I bands. For a bilayer of 1–2 dipalmitoyl-sn-glycero-3-phosphoglycerol (DPPG), the orientation and distribution of melittin (model for α-helical peptides) when interacting with the phospholipid bilayer could be elucidated using the amide I signals from SFG and ATR-FTIR measurements. The data were consistent with a dual δ-function distribution for the melittin orientation, where α-helical peptides may be parallel or perpendicular to the substrate when inserted in phospholipid bilayers [122]. The interaction between melittin and DPPG or deuterated DPPG (dDDPG) bilayers could also be monitored with real-time SFG measurements by following the C–H and C–D stretching signals [123].

Amyloid peptides have also been studied at lipid-aqueous interfaces, where their orientation was determined with SFG following the amide I band in *psp* polarization, which is specific to the contribution of chiral molecules, as shown in Fig. 6a [124]. The human islet amyloid polypeptide was found to be oriented at 48 ± 1° relative to the interface as shown in Fig. 6b, which was induced by the amphiphilic properties of the β-sheet aggregates with the peptide hydrophilic part exposed to the aqueous phase and the hydrophobic region to the lipid. This orientation suggests a potential disturbing effect on membrane integrity and may be the onset of diseases, such as Parkinson's disease and type II diabetes.

The conformation of peptides affects their interaction with lipids in membranes and vesicles, as one should expect, and this was proven with PM-IRRAS and FTIR by *Kouzayha* et al. [125]. Using the alanine-rich peptide $K_3A_{18}K_3$ and alamethicin, made to interact with DPPC monolayers and DMPC vesicles, *Kouzayha* et al. found that interaction should occur via the hydrophobic parts in α-helical peptides and via the hydrophilic parts in β-sheet peptides. The nonsteroidal anti-inflammatory drug meloxicam and its complex with β-cyclodextrin inhibited the enzymatic lipolysis of phospholipids in the membrane, as observed with PM-IRRAS, which could be related to their ability to prevent inflammatory processes [126].

The technological importance of lung surfactants has generated considerable work with Langmuir monolayers. Because DPPC and DPPG are the most abundant lipid components in the inner interface

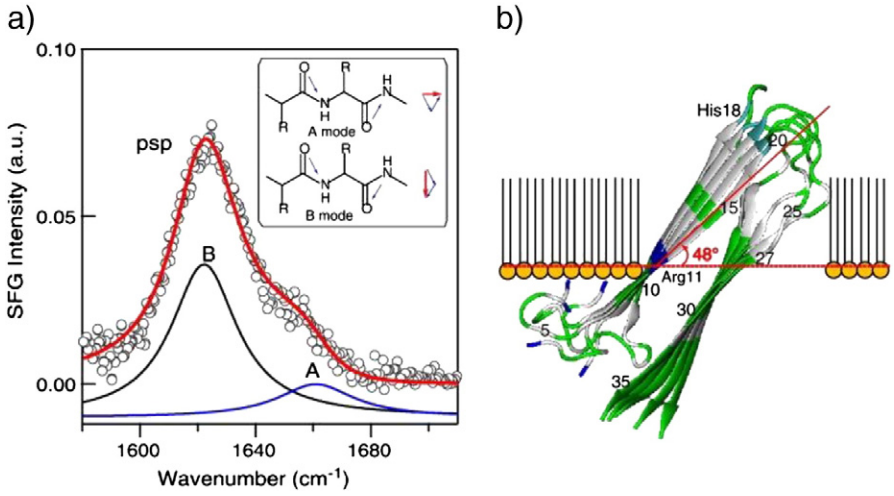

Fig. 6. (a) SFG spectra for the islet of amyloid polypeptide obtained at amide I region using *psp* polarization configuration (*p* — for SFG, *s* — for visible and *p* — for IR), which is specific for contribution of chiral molecules. (b) Orientation at 48 ± 1° relative to the interface when the amyloid polypeptide interacts with the lipid at the air–water interface. *Reprinted from* [124]. *Copyright 2014, with permission from Elsevier.*

of the lungs, they have been widely used in interaction studies [127], for which spectroscopic methods are ideally suited. *Flach* et al. [128] isolated a specific pulmonary protein from lung porcine to investigate, via IRRAS, the role of the two thioester-linked palmitoyl chains located near the N-terminus from deacylated protein SP-C. Deacylation of SP-C produced more fluid DPPC monolayers, with the helical-secondary structure and tilt-angle of the protein remaining essentially unchanged. A comparison of the secondary structure of surfactant proteins in bulk and at the air/water interface is important since these proteins facilitate replacing components across interfaces, which could be essential for in vivo functions in the alveolar subphase and at the air/alveolar interface [129]. *Dieudonne* et al. [129] used IRRAS to probe structure-function relationships and protein–lipid interaction in bulk phase and monolayer for three peptides with amino acid sequences based on the pulmonary surfactant protein SP-B (SP-B_{1-20}, SP-B_{9-36a} and SP-B_{40-60A}), with substantial differences being observed in peptide surface activity. The influence of tobacco smoke in clinical lung surfactants has been studied by using FTIR [130], where hydrophobic proteins from tobacco smoke-treated Survanta (a specific lung surfactant) affected the conformation of SP-B and SP-C.

3.1.1. Films deposited on solid substrates

As a complementary strategy to investigate protein interaction with cell membrane models, Langmuir–Blodgett (LB) films have been obtained with proteins adsorbed onto phospholipid monolayers. DMPA is one of the most used phospholipids in this context owing to its suitability to deposit multilayers [131,132]. Examples include studies of a mucin protein in LB films of DMPA, where chitosan was able to gradually remove the protein, according to FTIR measurements [116] and interaction studies between DMPA and the protein–polysaccharide complex extracted from the mushroom *Agaricus blazei* Murill [133]. The adsorption of horseradish peroxidase in DPPG films was explored to enhance its activity when compared with protein-containing solutions [134], where the protein was found to preserve its native structure when adsorbed onto DPPG. This type of information was obtained by analyzing PM-IRRAS spectra, with which the α-helix conformation of horseradish peroxidase in the phospholipid matrix was confirmed by monitoring its C═O and N – H groups.

In another example of cell membrane model with adsorbed films on solid substrates, *Wang* et al. [135] replaced an inorganic-lipid interface by an organic-lipid one. They examined and compared single lipid bilayers of DPPG and dDPPG assembled on solid surfaces of CaF_2 (inorganic-lipid interface) and on a poly(lactic acid) (PLLA) cushion (organic-lipid interface). With SFG they showed that the supported bilayers have similar structures, also interacting with an antimicrobial peptide in the same fashion. Fig. 7 depicts the experimental setup used to measure the PLLA-lipid bilayers interface interacting with the peptide Cecropin P_1. Because similar results to inorganic-lipid interacting with the peptide were obtained, the hydrophilic PLLA was found suitable to support lipid bilayers, which is important for studies involving transmembrane proteins, where the possible inorganic-lipid interactions may affect protein structure or function.

One important role of cell membranes is the ability to control charge transport from and to the cell, and this is mostly done by gating ion channels. This issue was addressed by *Chen* and co-workers [136], where the alamethicin peptide, which adopts $\alpha/3_{10}$-helix structure, interacted with palmitoyloleoylphosphatidyl choline (POPC) lipid bilayers deposited on CaF_2 substrates in the presence of an electric field created by changing the solution pH (an electric potential across the membrane). The localized pH change modulated the membrane potential and thus induced variations in both tilting angle θ (inclination of the peptide with respect to the normal to the plane) and bending angles φ of the helices in the peptide (angle between the two helical components in the peptide). This indicates the mechanism for opening the ion channel in living cells, which regulates ionic permeability through the membrane.

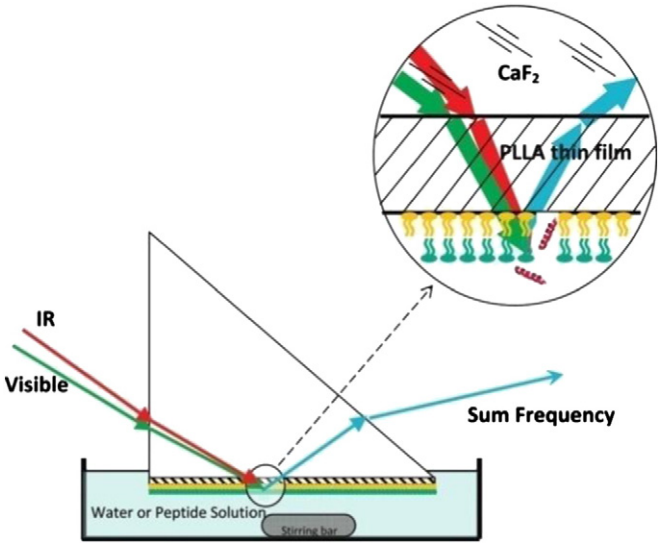

Fig. 7. SFG sample configuration used to study lipid bilayers deposited on solid surfaces of CaF_2 and PLLA exposed to water or peptide solutions. The inset shows the IR and visible beams crossing unwanted interfaces and reaching the desired one, where the SFG beam is generated. *Reprinted adapted with permission from* [135]. *Copyright 2014 American Chemical Society.*

Lipkowski and co-workers [137] also studied ion channels in supported bilayers mimicking cell-membrane using PM-IRRAS. A mixed bilayer containing 90% of DMPC and 10% of gramicidin (a well-known ion channel) was deposited onto a gold substrate. Upon applying an electrostatic potential to the gold electrode, they could switch states characterized by different packing and orientation of DMPC molecules and distinct orientations of the helix structures of gramicidin. With a more sophisticated molecular architecture to represent a cell membrane, the same group investigated the effects from binding cholera toxin to the membrane [138]. The first layer deposited on a gold substrate comprised DMPC and cholesterol, on top of which another layer was adsorbed which contained DMPC, cholesterol, monosialotetrahexosylganglioside (GM1) and a bound cholera toxin binding (CTB) unit. This latter layer was meant to model the outer (extracellular) leaflet of a cell plasma membrane. With PM-IRRAS being used to monitor the orientation of the fatty acid chains, Leitch et al. [138] showed that binding cholera toxin increased the tilt angle of the chains but did not affect the overall conformation of the bilayer to any great extent. The most important effect appears to be related to a significant voltage-dependent change in the opening of the CTB pore, which is governed by reorientation of the α-helix components of CTB. According to those authors, this finding is highly significant insofar as the pore opening mechanism may explain the transport of the toxin through the membrane [138].

LbL films have also been used to mimic cell membranes. *Pilbat* et al. [139] reported a method to immobilize cell membrane bilayers of DPPC in LbL films of poly-(glutamic acid)/poly(lysine) (PGA/PLL). The film growth regime was altered by inserting a DPPC bilayer in between the polyelectrolyte bilayers because this DPPC bilayer blocked diffusion for the next PGA/PLL layers. FTIR was used to monitor film growth and the immobilization of Gramicidin A on top of the LbL film, by following mainly the bands assigned to C – H stretching, amide I and amide II regions [140].

3.2. Probing surface functionalization

The immobilization of biomolecules onto solid substrates has been explored for two main targets, namely the immobilization of active molecules in biosensors and for fundamental studies on biocompatible surfaces. Early work on biosensors was performed by *Barraud* et al. [141], with the immobilization of the antibody immunoglobulin G on

fatty acid (ω-tricosenoic acid) LB films to detect *Staphylococcal enterotoxin B*. Film composition and the nature of antibody–fatty acid interactions were monitored with FTIR spectroscopy, with which the coverage ratio of the protein could be obtained. Indeed, the intensity of the absorption band at 1640 cm^{-1}, assigned to C═O groups from the protein, increased with the incubation time up to 60 min, when the coverage ratio reached a constant value of 60%. The influence from parameters such as pH, ionic strength, transfer pressure and antibody concentration in the subphase was also investigated. *Singhal* et al. [142] used FTIR to study immobilization of urease in mixed monolayers of poly(N-vinyl carbazole) and stearic acid, with the film being used in a biosensor for urea. Significantly, the urease in LB films did not lose its secondary structure, as indicated by probing the amide I and II bands of the enzyme. These amide bands were also useful to ensure the preservation of secondary structure for lysozyme adsorbed onto porous carbon sieves [143].

The detection of ethanol, which could be distinguished from its interferents, was achieved with a sensor array where one of the sensing units was made with immobilized alcohol dehydrogenase (ADH) in a matrix of negatively charged phospholipid DMPA, in an LB film [144]. ADH was incorporated from the subphase onto a DMPA Langmuir monolayer, and did not lose its native structure according to PM-IRRAS data for the amide I and II bands. PM-IRRAS was also essential to confirm that ADH remained at the air/water interface even at high surface pressures for the DMPA monolayer, thus making it possible to transfer onto a solid substrate in the form of an LB film containing both DMPA and ADH.

Since the control of molecular architecture may be essential to produce highly sensitive and selective biosensors, attempts have been made to combine more than one component in a given film. Obviously, such control can only be proven if suitable methods are available to interrogate the film architecture. This was performed with IRRAS to monitor immobilization of cholesterol oxidase (ChOx) and Prussian Blue (PB) in LB films of octadecyltrimethylammonium (ODTA) [145], whose structure is shown in Fig. 8. The incorporation of ChOx was confirmed by inspecting the amide I and II bands. With this LB film adsorbed on a Au-layer-patterned glass slide cholesterol could be detected using a conventional three-electrode electrochemical cell where PB was a redox mediator. The authors also reported a wide linear relationship between cholesterol concentration and the change in current density within the 0.2–1.2 mmol/L range, and they attributed it to the film structure formed by the LB technique, similarly to what was observed in glucose sensors based on ODTA/PB/GOx LB films [146].

Hydrogen bonding is crucial for many self-assembly processes, and FTIR spectroscopy is a prime method to monitor such interaction. *Pakalns* et al. [147] produced Arg-Gly-Asp (RGD) peptides by linking synthetic dialkyl tails in amino-terminus, carboxyl-terminus, and both termini of RGD. All of these amphiphilic peptides were able to self-assemble into stable monolayers with biologically active interfaces, but FTIR studies indicated that amino-coupled RGD head groups formed the strongest lateral hydrogen bonds. *Khopade* et al. [148] used FTIR spectroscopy to monitor the fabrication of crosslinked LbL multilayers of poly(styrenesulfonate) (PSS) and 4th generation poly(amidoamine) dendrimer (4G PAMAM), which were used in biocompatibility experiments with biological cells.

The functionalization of poly(ethylene terephthalate) at tertiary-amine-terminated allowed the immobilization of immunoglobin and horseradish peroxidase [149], where FTIR spectroscopy was employed to monitor the light-induced amination of poly(ethylene terephthalate) film. The attachment of amine groups increased with radiation time, which were able to anchor immunoglobin and horseradish peroxidase. FTIR spectroscopy was used to monitor immobilization of polyphenol oxidase in mesoporous activated carbon matrices [150], with the shifts in the bands assigned to polyphenol oxidase and the appearance of new bands pointing to stronger bonding with the functional groups of carbon matrices.

FTIR spectroscopy has been instrumental in studying the immobilization of biomolecules in conjunction with micro- and nanostructures that serve as templates. Microspheres of calcium carbonate/carboxymethyl cellulose were prepared to support lysozyme [151], alcohol dehydrogenase was immobilized on oxidized diamond nanoparticles [152] and superparamagnetic carboxymethyl chitosan nanoparticles were utilized on the immobilization of trypsin [153]. In all of these cases, FTIR was important not only to confirm immobilization with the presence of amides I and II bands but also to identify the enzyme structure adopted.

Various strategies are used to prevent denaturing of biomolecules when they are immobilized onto solid supports. For instance, the ordered structure adopted by *it*-PMMA/*at*-PMMA (poly(methyl methacrylate) LbL films made it possible to immobilize β-galactosidase with preserved activity, in contrast to the case of single-component films coating partially ordered *it*-PMMA or disordered *at*-PMMA, for which β-galactosidase would be denatured [154]. Information on protein denaturing and adsorption was obtained with ATR–IR spectroscopy, and the cartoon in Fig. 9 depicts the findings.

In many cases, vibrational spectroscopy is a key to determine whether adsorption occurred. For example, the deposition of LbL films of a phospholipid polymer PMVB (synthesized from 2-methacrylocyloxyethyl phosphorylcholine, n-butyl methacrylate, and 4-vinylphenylboronic acid) and poly(vinyl alcohol) (PVA) on Ti substrates was performed for improving the biocompatibility of implants [155], and adsorption was confirmed using ATR–FTIR spectra taken from the outer layer during film fabrication. The PMBV/PVA LbL films on the Ti substrate suppressed the adhesion of L929 cells (cultured in a culture medium — D-MEM Gibco), compared with that on an untreated Ti, being therefore promising for improving biocompatibility of Ti-based medical devices.

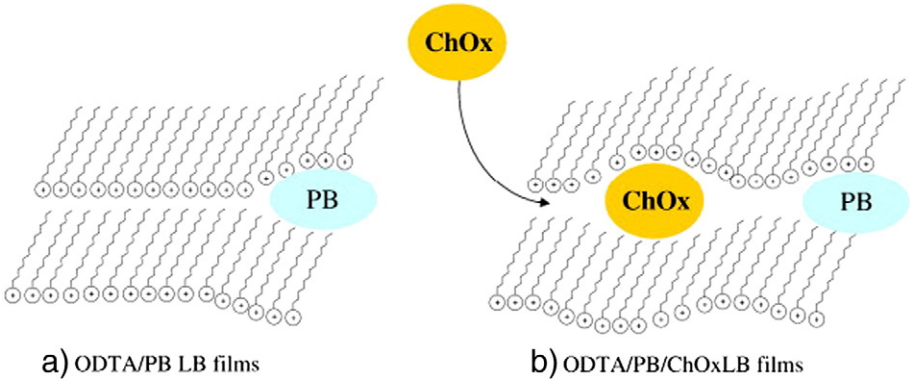

Fig. 8. Models for incorporation of (a) PB, and (b) PB and ChOx in ODTA LB films. ChOx was immobilized on the LB films by immersing them in an aqueous solution, and immobilization was confirmed by IRRAS measurements in the spectral range of amides I and II. *Reprinted adapted with permission from* [146]. *Copyright 2014 American Chemical Society.*

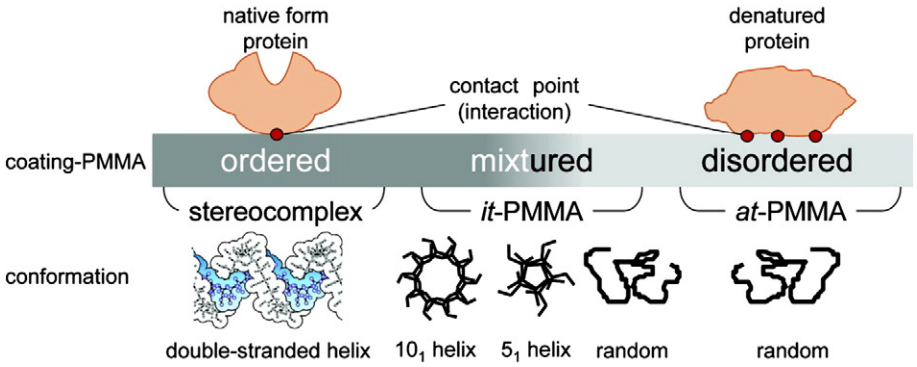

Fig. 9. The influence of the ordered structure *it*-PMMA/*at*-PMMA, partially ordered structure *it*-PMMA and disordered structure *at*-PMMA on the immobilization of the enzyme β-galactosidase. The enzyme can adopt different structures by varying the ordering of the molecules on the substrate. The red circles represent the interaction between the enzyme and substrate. *Reprinted adapted with permission from* [149]. *Copyright 2014 American Chemical Society*.

Surface coatings are now used for biosensing, especially for detecting low levels of analytes in biological media [156], in many cases exploiting plasmonic effects. In this review paper we shall concentrate on SERS applied to biological systems, as in the possible coating of nanoparticles with lipid liposomes for biomedical diagnostics [157]. Lipids are promising coatings for particles because of their biocompatibility, ability to self-assemble into organized structures and potential to stabilize metal nanoparticles. The lipid-encapsulated nanoparticles have been shown stable for weeks [157]. The versatility of the lipid layer was proven by incorporation of three SERS-active probes (malachite green, tryptophan, and Lissamine rhodamine DSPE) into the membrane to verify the efficiency of the lipid-encapsulated nanoparticles as SERS-active surfaces. The lipid layer was directly observed by transmission electron microscopy (TEM), and the incorporation of the three dye species was confirmed by SERS, as shown in Fig. 10. In a similar strategy, triangular AgNPs were coated with chitosan [156], which is a biocompatible shell to AgNPs [158].

Lipids, proteins and small molecules in the cell membrane are known to present affinity towards binding nanoparticles [90]. *Hodges* et al. [159] reported an immunolabeling protocol based on Au-conjugated antibodies combined with AgNPs for obtaining biomolecular information of the cell surface. The model system was the corneal endothelium whose apical surface is readily accessible for antibody labeling. Fig. 11 shows a schematic representation of AgNPs attached to the cell achieving the SERS effect of the cell membrane components. The nanoparticles were not modified with any SERS probe, which might have decreased the sensitivity but the enhanced signal comes solely from the immediate environment around the nanoparticle.

A highly sensitive optical imaging method was developed by *Lee* et al. [160], where the advantages of SERS and fluorescence spectroscopy were combined in a dual mode nanoprobe (DMNP). Fig. 12a shows the fabrication process of the SERS-fluorescence DMNP, detailed as follows: (i) synthesis of 40 nm AuNPs and (ii) adsorption of malachite green isothiocyanate (MGITC) and tris(2,20-bipyridyl)ruthenium(II) chloride hexahydrate (Rubpy) Raman reporters onto their surface. (iii) The Raman reporter-labeled AuNPs were encapsulated with a silica shell to prevent the release of Raman reporter molecules. In addition, the thickness of the silica shell was tuned to achieve the maximum intensity of the fluorescent dye (fluorescent ITC-modified with FITC or RuITC) covalently attached onto their surface (iv). The nanostructures were encapsulated with a final silica shell (v) in order to minimize nanoparticle aggregation and to protect the fluorescent dye. DMNP was further attached to specific antibodies for targeting and imaging specific breast cancer markers in living cells, as displayed by the schematic outline in Fig. 12b. The final geometry of the nanostructure allows one to collect fluorescence signal as a fast track tool for the recognition of cancer markers, in addition to SERS as an accurate tool for imaging localized marker distributions [161,162]. In a related work, an aqueous-phase immunoassay protocol was developed with the SERS-fluorescence DMNP and magnetic nanobeads [163].

Jiang et al. [155] brought together dark field images and SERS taking advantage of Au modified nanorods. Raman reporter molecules were chemically attached to the nanorods through Au–S or Au–N interactions. Polyelectrolyte multilayers of poly(allylaminehydrochloride) (PAH) and poly(styrenesulfonate) (PSS) were further assembled onto nanoparticle surfaces to reach better stability and biocompatibility. Finally, ligands for commonly overexpressed receptors on tumors (carcinoembryonic antibody or transferrin) were electrostatically adsorbed onto polyelectrolyte coatings. A diagram illustrating the preparation of Au nanorods coated with the Raman reporter and

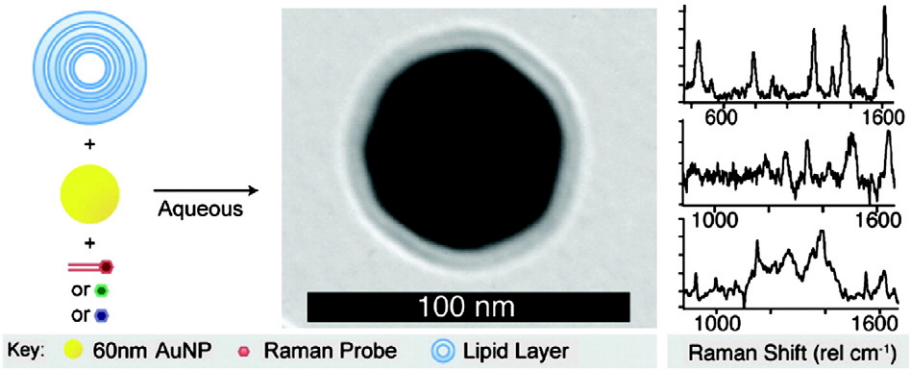

Fig. 10. Illustration of the lipid-encapsulated gold nanoparticles. The solid circle represents the gold nanoparticle, the rings represent lipid layers, and the small hexagons represent dye molecules. Also shown are the TEM image of the lipid-encapsulated gold nanoparticles and the SERS spectra of Malachite green (1), rhodaminelissamine DSPE (2), and tryptophan (3). *Reprinted adapted with permission from* [157]. *Copyright 2014 American Chemical Society*.

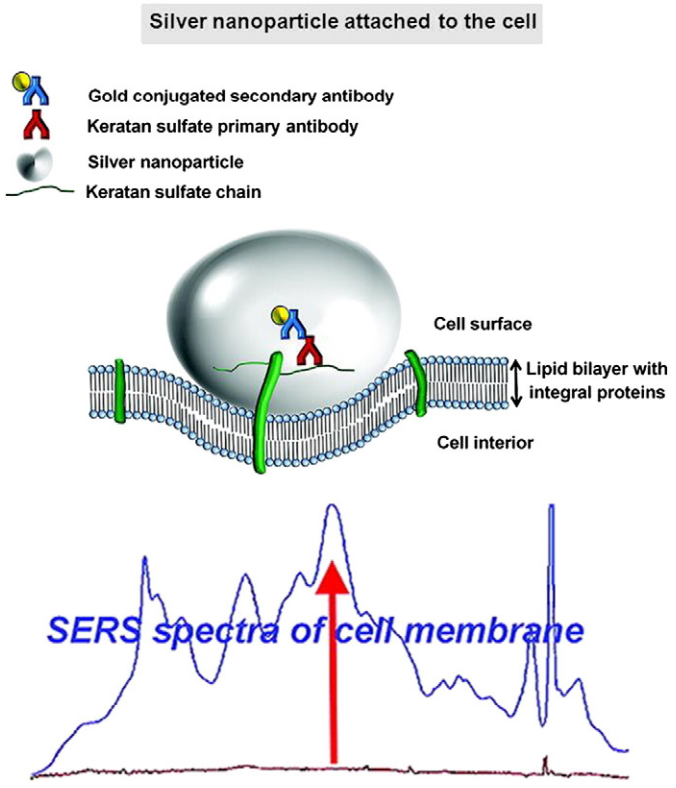

Fig. 11. Schematic representation of AgNPs attached to the cell achieving the SERS effect of the cell membrane components. *Reprinted adapted with permission from* [159]. *Copyright 2014 American Chemical Society*.

polyelectrolytes (PAH and PSS) layers is shown in Fig. 13. HeLa cells were chosen as target cancer cells in the experiment. The modified nanorods uptaken by cancer cells provide not only dark field cell images but also SERS images recorded by the unique signal of the Raman reporter, as shown in Fig. 13b and c. The designed nanostructures are potentially useful for in vivo bioimaging and photothermal therapy of cancer cells [164].

Plasmon resonance Rayleigh scattering (PRRS) and SERS were combined with AgNPs to analyze the influence of mannoproteins on yeast cell wall surfaces with an inhibition assay [165], making it possible to detect single nanoparticles. SERS is able to distinguish the Rayleigh scattering of the nanoparticles and cell components, bringing the vibrational information of the system under analysis. Despite the lack of SERS reproducibility pointed out by the authors, PRRS and SERS can be joined in a powerful method for highly sensitive, non-invasive analysis of cell surfaces.

An additional use of spectroscopic techniques is in understanding the adsorption mechanisms in films with two or more components, in which synergy is sought as is the case of many LbL films. Of particular relevance is the molecular-level interaction between components which may lead to completely distinctive properties of the final film in comparison to those of the individual components. For instance, *Aoki* et al. [166] immobilized DPPG vesicles onto PAH layers using the LbL technique. FTIR spectroscopy revealed that the interactions between NH_3^+ (PAH) and PO_4^- (DPPG) groups are the main driving forces for the PAH/DPPG LbL film growth. A similar strategy was applied to produce LB films containing multilayers of DPPG [167]. In the spirit of the electrostatic LbL technique, DPPG multilayer LB films were produced by transferring DPPG Langmuir monolayers from the water subphase containing low concentrations of PAH onto solid substrates. Once again, the goal was to take advantage of NH_3^+ (PAH) and PO_4^- (DPPG) electrostatic interactions to grow LB multilayers of PAH/DPPG. Despite the same molecular-level interaction, the films obtained with the LB and LbL techniques displayed distinct molecular architectures since DPPG was structured as monolayers in the LB films and as vesicles in the LbL films. There are cases, however, where such molecular-level interaction is not observed, in spite of the intimate contact in LbL films. Indeed, *Moraes* et al. [168] obtained FTIR spectra for LbL films made with DPPG liposomes alternated with layers of poly(amidoamine) G4 (PAMAM) dendrimer, which were the mere sum of the spectra of PAMAM and DPPG.

As mentioned before, SFG spectroscopy can probe ordering of hydrocarbon chains as well as the head functional groups of monolayers. The growth and adhesion of cortical neurons on self-assembled monolayers depends on the functional groups for amino-terminated, carboxy-terminated and 1:1 mixed alkanethiol monolayers on gold, as described by *Palyvoda* et al. [169]. Using SFG they inferred that the ordering of the terminal amino groups does not affect the ability for neuron adhesion, while the dissociation of carboxylic groups hampers neuron attachment. They reported that a net overall positive charge on the surface is crucial to the neuronal adhesion, being amino groups very effective adhesion promoters, while the surface carboxyl groups which are negatively charged presented no ability to bind neurons. The role played by surface roughness was also studied, using gold substrates with mean roughness 1.9 nm (type A) and 0.7 nm (type B). Fig. 14 shows CO stretching bands assigned to the −COOH group at 1767 cm^{-1} (*iii* vibrational mode in the figure) and at 1654 cm^{-1} assigned to asymmetric CO stretching from the anionic COO− group (*i* vibrational mode). In the pure carboxy-teminated SAMs (spectra C and D), the 1767 cm^{-1} stretching band is broad for type A gold substrate (spectrum C) and more easily distinguished for type B gold (spectrum D). This indicates increasing order of the terminal carboxy groups deposited on the low roughness gold type B. Moreover, the bands for mixed SAMs (spectra A and B) were stronger and narrower than those for pure carboxy-

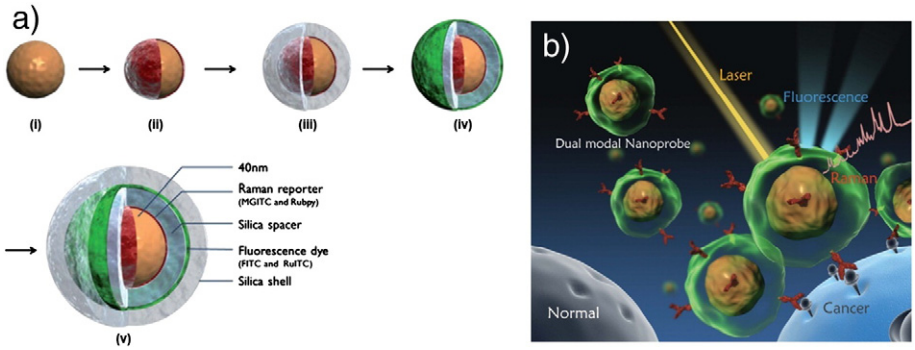

Fig. 12. (a) Fabrication process of the SERS-fluorescence DMNP and (b) schematic outline displaying cancer marker detection using SERS-fluorescence DMNP. Fast tracking is allowed by fluorescence, and SERS provides detailed information about molecular interactions and imaging of localized marker distributions. *Reprinted adapted with permission from* [160]. *Copyright 2014 American Chemical Society*.

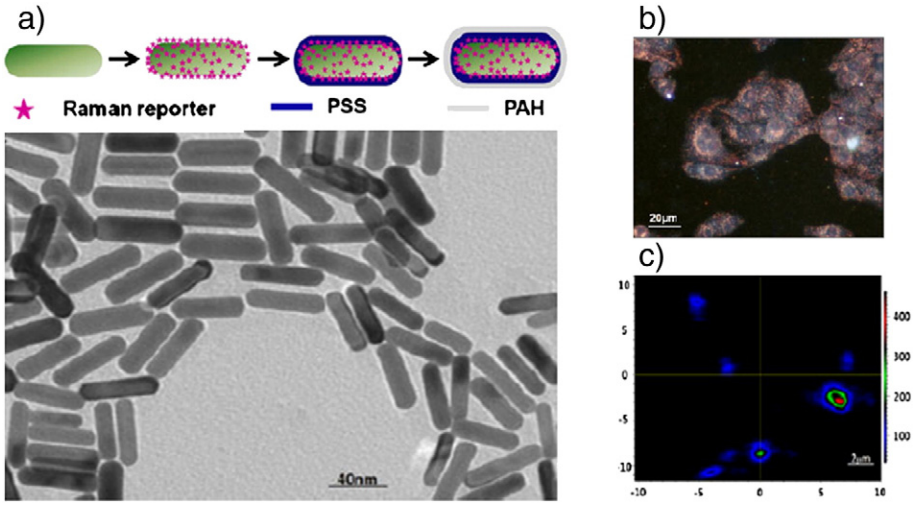

Fig. 13. (a) Diagram illustrating the preparation of Au nanorods coated with Raman reporter and polyelectrolyte (PAH and PSS) layers. The morphology of the modified nanorods is shown by the TEM image. Dark field (b) and SERS (c) images of HeLa cells marked with the modified nanorods. *Reprinted from* [164]. *Copyright 2014, with permission from Springer.*

terminated SAMs, revealing that mixing of carboxy- and amino terminated SAMs also causes better ordering of the terminal groups.

A further advantage of the SFG method is the possible quantitative analysis it provides, as shown by previous examples (Section 3.1). *Ye* et al. [170] made use of SFG with varying polarization of the light impinging onto the samples to quantitatively probe peptide orientations adsorbed on polymer surfaces coated on solid CaF_2 substrates. They used polystyrene (PS) and polystyrene maleimide (PS-MA) and the Cysteine-terminated cecropin P1 (CP1) as a probe peptide whose amide I and II bands were monitored. Differences in orientation could be noted between physically adsorbed and chemically immobilized CP1c on the polymer surfaces. Furthermore, the peptide orientation also depended on whether it was in air or water, as demonstrated by measurements with the films exposed to air or exposed to buffer solutions or water.

Hybrid LB films have been produced with the proteins lysozyme and bovine serum albumin being incorporated in films containing saponite,

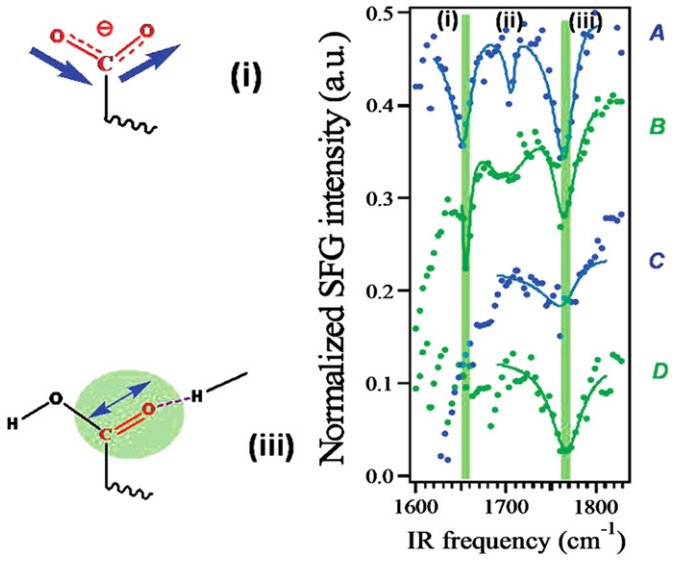

Fig. 14. SFG spectra obtained using the *ppp* polarization configuration for mixed SAMs deposited on gold (A) type A and (B) type B, and neat SAMs of 10-carboxy-1-decanethiol deposited on gold (C) type A and (D) type B. The two main vibrational modes are (i) 1654 cm^{-1} assigned to stretching of COO− group and (iii) 1767 cm^{-1} assigned to stretching of −COOH group. *Reprinted adapted with permission from* [169]. *Copyright 2014 American Chemical Society.*

where the presence of the latter could be confirmed in ATR–FTIR spectra with the S–O in-plane vibration band at 1000 cm^{-1} while the characteristic amide I and II bands confirmed the presence of the proteins [171]. Significantly, both proteins had their native structure preserved, and stronger adsorption was observed for the positively charged lysozyme since saponite was negatively charged. Another type of hybrid film was made with carbon nanotubes (CNTs) incorporated from their suspensions into an LB film of 4-nitro-3-(octanoyloxy)benzoic acid – OBZ – in stearic acid [172]. These films affected the activity of phospholipase A_2 isolated from *Crotalus durissus cumanensis*, according to PM-IRRAS data. It was concluded that CNTs created a new molecular accommodation for the enzymatic action on the film surface and preserving enzyme activity.

Two-dimensional surface-enhanced IR absorption spectroscopy (2D SEIRAS) in the ATR-mode was used to monitor the catalytic activity of Cytochrome c oxidase (CcO) immobilized on a tethered bilayer lipid membrane deposited on a gold support [173]. With potentiometric titrations of CcO, differences could be noted between the non-activated and the activated states of the enzyme, as indicated by changes in the 2D SEIRA spectra as the electric potential was varied. These states could be correlated to different conformations of CcO.

In a pioneering work, *Brolo* and coworkers used PM-IRRAS in conjunction with surface-enhanced (resonance) Raman scattering (SERRS) to monitor the fabrication of a biofuel cell anode [174]. The anode was built with deposition of a monolayer of 4-hydroxythiophenol (HTP) attached to a coenzyme cibacron blue F3G-A (CB), which is suitable for incorporation of the enzyme formaldehyde dehydrogenase (FalDH). The HTP-coated Au electrode (also used as SERS substrate or gold film used for PM-IRRAS) was immersed in a CB solution for adsorption of the coenzyme, forming the layered structure Au/HTP/CB. FalDH was adsorbed via drop-coating, leading to the anode architecture Au/HTP/CB/FalDH illustrated in Fig. 15. The fabrication process was monitored as follows. Upon adsorbing HTP on Au the S–H band observed in the spectrum of bulk HTP was missing because the S atoms from HTP were bonded to the Au atoms from the electrode. The incubation of FalDH on the Au/HTP/CB architecture altered the CB bands, with the relative intensities of the ~1400 and ~1580 cm^{-1} bands being changed and the 1636 cm^{-1} band shifted to a higher frequency. This indicated that the enzyme was chemically bonded to CB.

4. Strengths and limitations of the spectroscopic methods

All techniques described here (SERS, (PM-)IRRAS and SFG) have the capability of obtaining vibrational spectra of interfacial molecules,

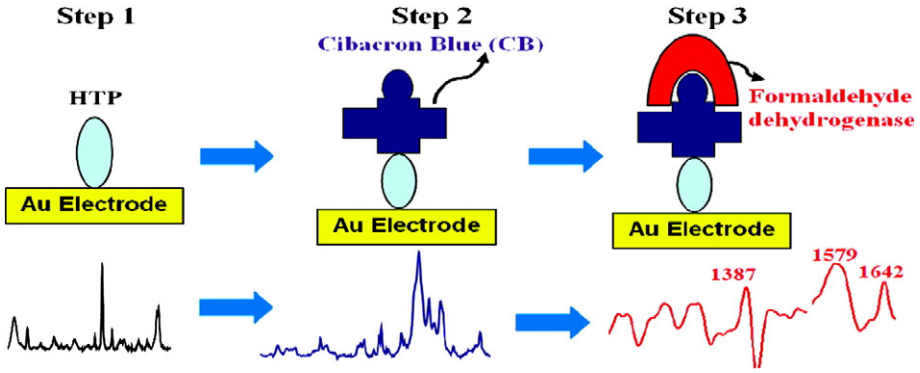

Fig. 15. Surface-enhanced (resonance) Raman scattering (SERRS) and PM-IRRAS used to monitor the construction of a biofuel cell anode. The depositions of HTP onto gold (Step 1), CB onto HTP (Step 2) which is suitable for enzyme incorporation, and the enzyme FalDH onto CB (Step 3) were monitored using these spectroscopic techniques. *Reprinted adapted with permission from* [174]. *Copyright 2014 American Chemical Society*.

which in turn can be used to deduce information on the molecular level about structure and interactions at interfaces. Each one has its particular strengths and limitations, so that usually a combination of these methods may yield the best results.

Surface infrared spectroscopy (ATR, IRRAS and PM-IRRAS) is now a widespread technique for investigating biomimetic interfaces, such as Langmuir and LB films. Among its advantages one can mention a simpler and lower cost experimental setup, high sensitivity, capability of in situ and real-time experiments to observe adsorption dynamics, and the possibility of obtaining information on molecular orientation. However, it has a limited specificity to interfaces, and contribution of bulk molecules to the IRRAS spectra may be significant, even in the attenuated total internal reflection geometry (ATR-IRRAS), where the penetration depth of the IR radiation may be a few hundred nm. Even with polarization modulation (PM-IRRAS), it is not clear that the bulk contribution is completely suppressed. For weak signals, these techniques also suffer from problems associated with baseline correction, which may lead to distorted bandshapes or incorrect intensities. One difficulty for using infrared absorption-based techniques which remains is associated with the bending bands of water, for they generally overlap with amide I bands of biomaterials.

SFG spectroscopy has several advantages with respect to other techniques. The most important is its extreme surface selectivity, which makes it possible to probe, for example, the surface structure of pure liquids and solutions [102], or water interacting with Langmuir films [78]. Furthermore, it has high sensitivity, leads to usually simpler vibrational spectra due to its stringent selection rule (modes must be both IR- and Raman-active), it is non-destructive and capable of in situ and real-time experiments. It is also generally possible to obtain qualitative information on molecular orientation, and in many cases a quantitative analysis is feasible, although in this case it usually relies on several parameters and models for the nonlinear response of the molecules that may be poorly known. One interesting aspect of SFG spectroscopy with regard to biomembrane mimetic systems is its ability to qualitatively probe lipid chain conformation with high sensitivity. This can also be probed with IR spectroscopy, but it usually relies on small frequency shifts (a few cm^{-1}) or slight broadening of CH_2 stretches [175,176], which may be difficult to observe in weak signals. With SFG, conformational changes in lipid chains lead to changes in the ratio of intensities for CH_2 and CH_3 stretches, a much more sensitive and compelling evidence [76]. Detection of molecular chirality is also quite simple and sensitive with SFG [80,124]. Finally, the possibility of SFG imaging of interfaces, with chemical (vibrational spectroscopy) and orientational sensitivities, and good spatial resolution (a few μm) has been demonstrated in the last decade [177,178]. Even near-field (~100 nm) resolution SFG imaging has been accomplished, but with quite limited sensitivity [179]. The major drawback of SFG spectroscopy is a relatively complex and costly experimental setup. Additionally, since it is a coherent nonlinear optical process, the vibrational lineshapes may be complicated by interference with nonresonant contributions or nearby resonances, which makes data analysis and interpretation more involved. These two factors still prevent a wider applicability of SFG spectroscopy. Other important limitations of the SFG technique are: it can only probe non-centrosymmetric molecules, the need of flat (optically reflecting) interfaces, and the possibility of optical damage to the samples due to high laser intensities.

The SERS technique is advantageous in comparison to other methods for analytical tasks, including extremely high sensitivity, inherent molecular specificity of unlabeled targets, no water interferences, narrow spectral bands, and being also non-destructive and non-invasive. It may be applied in-situ and in-vitro for biological samples, and works under a wide range of temperature and pressure conditions [180]. For biosensing and diagnosis, the major advantage of SERS over electrical or electrochemical biosensors is in the absence of interference from background conductivities and non-specific binding [180]. In relation to other optical techniques such as surface plasmon resonance (SPR), SERS can be used as a specific measurement while SPR is based on the measure of mass accumulation, in which changes due to molecules non-specifically bound cannot be differentiated from the target. With respect to fluorescence techniques, besides the photostability (photobleaching of fluorescent probes), SERS presents simpler sample preparation [180]. Among SERS' important features are molecular identity (fingerprint spectrum), information about 3D structural changes (orientation, conformation) and intermolecular interactions. Furthermore, of the three techniques discussed here, SERS is the only one that allows high-resolution imaging with chemical (vibrational) information. Typical spatial resolution in micro-Raman instruments is ~1 μm, while for SFG microscopy and IR microscopy it varies in the range of about 5 to 20 μm.

5. Conclusion and future prospects

The many examples for the use of spectroscopy methods in cell membrane models and surface functionalization presented here are indication that such techniques will become increasingly prevalent in various areas of materials science, physical chemistry, biophysics and biochemistry. We have concentrated on applications for nanostructured films containing molecules of biological interest, which are used to mimic biointerfaces, but the spectroscopy methods are also relevant for any other type of interface. A crucial step in the next few years is to disseminate the methods to health and life sciences, particularly to assist in the design of new drugs and understanding physiological action depending on interactions with cell membranes, and in the identification of new opportunities for diagnosis and therapy based on surface coatings. This will require close cooperation with professionals from other fields, especially physicists and chemists.

With regard to prospects associated with the methods themselves, for SFG spectroscopy we envisage both technological and theoretical/experimental advances. On the former, although commercial SFG spectrometers are available, it would be interesting to develop compact, lower-cost and user-friendly SFG setups, so that the technique may be more widely used, even by non-specialists. This would be important to make the technique available to biomedical researchers for in vivo investigations. On the theoretical side, it would be helpful to have calculations of the nonlinear ($\chi^{(2)}$) vibrational response of molecules, which would allow more reliable determination of molecular orientation [124], and simulations of the SFG spectra, which would greatly facilitate obtaining structural information from the vibrational spectra [181]. Two aspects of SFG spectroscopy that have already been demonstrated remain to be further explored in the context of biomimetic systems: SFG imaging [177,178] and SFG scattering [182]. For example, SFG imaging of lipid domains (rafts) in mixed films, bilayers or real membranes would be very interesting, and could bring additional molecular-level information such as conformation, interaction and orientation. The extension to non-planar surfaces by SFG scattering is indeed very promising, since a greater variety of systems could be investigated, including functionalized liposomes or colloidal particles, which include the effect of curvature and would be better models for cell membranes.

A more widespread use of PM-IRRAS will also depend on the development of less costly equipment and software for data analysis. In terms of determining the structure of biomolecules at the interfaces, it is probably the most versatile method currently available, though other IR absorption methods have also performed well in this regard [183,184]. As for SERS, the theoretical background has been firmly established, but in terms of experimental setups three main challenges remain: i) to design and produce reliable and reproducible SERS-substrates. The latter is intimately related to the development of nanotechnology regarding templates and metallic nanoparticles, which could allow one to obtain SERS-substrates with predictable enhancement factors. This is a necessary step to make SERS a routine analytical technique. ii) to understand the possible interaction between metallic nanoparticles and the system under investigation, for chemisorption could affect the sample, especially in biological samples for which the nanoparticles could be toxic. iii) to reach single molecule detection in routine procedures, rather than on limited conditions as it is today. A first step in such direction was made with the use of computational techniques related to information visualization to improve the spectral analysis [185].

Acknowledgments

This work was supported by FAPESP, CNPq, CAPES and the nBioNet network (Brazil).

References

[1] Kasemo B. Biological surface science. Surf Sci 2002;500:656–77.
[2] The 4th International Symposium on Surface and Interface of Biomaterials Rome, Italy; 2013.
[3] Lutolf MP, Hubbell JA. Synthetic biomaterials as instructive extracellular microenvironments for morphogenesis in tissue engineering. Nat Biotechnol 2005;23:47–55.
[4] E.F. Bernstei, P.L. Blackshe, Keller KH. Factors influencing erythrocyte destruction in artificial organs. Am J Surg 1967;114:126.
[5] Colton CK. Implantable biohybrid artificial organs. Cell Transplant 1995;4:415–36.
[6] Desai TA. Micro- and nanoscale structures for tissue engineering constructs. Med Eng Phys 2000;22:595–606.
[7] Bridgewater K. Achievements and advances for artificial organs. Artif Organs 2013;37:499–500.
[8] Grundfest-Broniatowski S. What would surgeons like from materials scientists? Wiley Interdiscip Rev Nanomed Nanobiotechnol 2013;5:299–319.
[9] Boyan BD, Hummert TW, Dean DD, Schwartz Z. Role of material surfaces in regulating bone and cartilage cell response. Biomaterials 1996;17:137–46.
[10] Hollister SJ. Porous scaffold design for tissue engineering. Nat Mater 2005;4:518–24.
[11] Niklason LE, Gao J, Abbott WM, Hirschi KK, Houser S, Marini R, et al. Functional arteries grown in vitro. Science 1999;284:489–93.
[12] Stevens MM, George JH. Exploring and engineering the cell surface interface. Science 2005;310:1135–8.
[13] Cui HG, Webber MJ, Stupp SI. Self-assembly of peptide amphiphiles: from molecules to nanostructures to biomaterials. Biopolymers 2010;94:1–18.
[14] Muzzarelli RAA. Chitins and chitosans for the repair of wounded skin, nerve, cartilage and bone. Carbohydr Polym 2009;76:167–82.
[15] Petersen TH, Calle EA, Zhao LP, Lee EJ, Gui LQ, Raredon MB, et al. Tissue-engineered lungs for in vivo implantation. Science 2010;329:538–41.
[16] Zhang LJ, Webster TJ. Nanotechnology and nanomaterials: promises for improved tissue regeneration. Nano Today 2009;4:66–80.
[17] Gomes S, Leonor IB, Mano JF, Reis RL, Kaplan DL. Natural and genetically engineered proteins for tissue engineering. Prog Polym Sci 2012;37:1–17.
[18] Kamaly N, Xiao ZY, Valencia PM, Radovic-Moreno AF, Farokhzad OC. Targeted polymeric therapeutic nanoparticles: design, development and clinical translation. Chem Soc Rev 2012;41:2971–3010.
[19] Seliktar D. Designing cell-compatible hydrogels for biomedical applications. Science 2012;336:1124–8.
[20] Nel AE, Madler L, Velegol D, Xia T, Hoek EMV, Somasundaran P, et al. Understanding biophysicochemical interactions at the nano-bio interface. Nat Mater 2009;8:543–57.
[21] Huang HJ, Pierstorff E, Osawa E, Ho D. Protein-mediated assembly of nanodiamond hydrogels into a biocompatible and biofunctional multilayer nanofilm. ACS Nano 2008;2:203–12.
[22] Mora-Huertas CE, Fessi H, Elaissari A. Polymer-based nanocapsules for drug delivery. Int J Pharm 2010;385:113–42.
[23] Siepmann F, Siepmann J, Walther M, MacRae RJ, Bodmeier R. Polymer blends for controlled release coatings. J Control Release 2008;125:1–15.
[24] Zelikin AN. Drug releasing polymer thin films: new era of surface-mediated drug delivery. ACS Nano 2010;4:2494–509.
[25] Chaki NK, Vijayamohanan K. Self-assembled monolayers as a tunable platform for biosensor applications. Biosens Bioelectron 2002;17:1–12.
[26] Katz E, Willner I. Probing biomolecular interactions at conductive and semiconductive surfaces by impedance spectroscopy: routes to impedimetric immunosensors, DNA-Sensors, and enzyme biosensors. Electroanalysis 2003;15:913–47.
[27] Kharitonov AB, Zayats M, Lichtenstein A, Katz E, Willner I. Enzyme monolayer-functionalized field-effect transistors for biosensor applications. Sens Actuators B 2000;70:222–31.
[28] Kang XH, Wang J, Wu H, Aksay IA, Liu J, Lin YH. Glucose oxidase–graphene–chitosan modified electrode for direct electrochemistry and glucose sensing. Biosens Bioelectron 2009;25:901–5.
[29] Srivastava RK, Srivastava S, Narayanan TN, Mahlotra BD, Vajtai R, Ajayan PM, et al. Functionalized multilayered graphene platform for urea sensor. ACS Nano 2012;6:168–75.
[30] Wong-Ekkabut J, Baoukina S, Triampo W, Tang IM, Tieleman DP, Monticelli L. Computer simulation study of fullerene translocation through lipid membranes. Nat Nanotechnol 2008;3:363–8.
[31] Cai KY, Frant M, Bossert J, Hildebrand G, Liefeith K, Jandt KD. Surface functionalized titanium thin films: zeta-potential, protein adsorption and cell proliferation. Colloids Surf B Biointerfaces 2006;50:1–8.
[32] Iwasaki Y, Saito N. Immobilization of phosphorylcholine polymers to Ti-supported vinyldimethylsilyl monolayers and reduction of albumin adsorption. Colloids Surf B Biointerfaces 2003;32:77–84.
[33] Satriano C, Fragala ME, Aleeva Y. Ultrathin and nanostructured ZnO-based films for fluorescence biosensing applications. J Colloid Interface Sci 2012;365:90–6.
[34] Wong JY, Majewski J, Seitz M, Park CK, Israelachvili JN, Smith GS. Polymer-cushioned bilayers. I. A structural study of various preparation methods using neutron reflectometry. Biophys J 1999;77:1445–57.
[35] Fragneto-Cusani G. Neutron reflectivity at the solid/liquid interface: examples of applications in biophysics. J Phys Condens Matter 2001;13:4973–89.
[36] Irvine DJ, Mayes AM, Satija SK, Barker JG, Sofia-Allgor SJ, Griffith LG. Comparison of tethered star and linear poly(ethylene oxide) for control of biomaterials surface properties. J Biomed Mater Res 1998;40:498–509.
[37] Krueger S, Meuse CW, Majkrzak CF, Dura JA, Berk NF, Tarek M, et al. Investigation of hybrid bilayer membranes with neutron reflectometry: probing the interactions of melittin. Langmuir 2001;17:511–21.
[38] Ge CC, Du JF, Zhao LN, Wang LM, Liu Y, Li DH, et al. Binding of blood proteins to carbon nanotubes reduces cytotoxicity. Proc Natl Acad Sci U S A 2011;108:16968–73.
[39] Hama H, Kurokawa H, Kawano H, Ando R, Shimogori T, Noda H, et al. Scale: a chemical approach for fluorescence imaging and reconstruction of transparent mouse brain. Nat Neurosci 2011;14 [1481-U166].
[40] Qian XM, Nie SM. Single-molecule and single-nanoparticle SERS: from fundamental mechanisms to biomedical applications. Chem Soc Rev 2008;37:912–20.
[41] Qian XM, Peng XH, Ansari DO, Yin-Goen Q, Chen GZ, Shin DM, et al. In vivo tumor targeting and spectroscopic detection with surface-enhanced Raman nanoparticle tags. Nat Biotechnol 2008;26:83–90.
[42] Fu L, Ma G, Yan ECY. In situ misfolding of human islet amyloid polypeptide at interfaces probed by vibrational sum frequency generation. J Am Chem Soc 2010;132:5405–12.
[43] Mondal JA, Nihonyanagi S, Yamaguchi S, Tahara T. Structure and orientation of water at charged lipid monolayer/water interfaces probed by heterodyne-detected vibrational sum frequency generation spectroscopy. J Am Chem Soc 2010;132:10656–7.
[44] Shaffer MF, Dingel JH. A study of antigens and antibodies by the monolayer film technique of Langmuir. Proc Soc Exp Biol Med 1938;38:528–30.

[45] Maget-Dana R. The monolayer technique: a potent tool for studying the interfacial properties of antimicrobial and membrane-lytic peptides and their interactions with lipid membranes. Biochim Biophys Acta Biomembr 1999;1462:109–40.
[46] McConnell HM. Structures and transitions in lipid monolayers at the air–water-interface. Annu Rev Phys Chem 1991;42:171–95.
[47] Germer LH, Storks KH. The structure of Langmuir–Blodgett films of stearic acid. Proc Natl Acad Sci U S A 1937;23:390–7.
[48] Czolkos I, Jesorka A, Orwar O. Molecular phospholipid films on solid supports. Soft Matter 2011;7:4562–76.
[49] Decher G. Fuzzy nanoassemblies: toward layered polymeric multicomposites. Science 1997;277:1232–7.
[50] Lvov Y, Ariga K, Ichinose I, Kunitake T. Assembly of multicomponent protein films by means of electrostatic layer-by-layer adsorption. J Am Chem Soc 1995;117:6117–23.
[51] Tang Z, Wang Y, Podsiadlo P, Kotov NA. Biomedical applications of layer-by-layer assembly: from biomimetics to tissue engineering. Adv Mater 2006;18:3203–24.
[52] Barth A, Zscherp C. What vibrations tell us about proteins. Q Rev Biophys 2002;35:369–430.
[53] Greenler RG. Infrared study of adsorbed molecules on metal surfaces by reflection techniques. Journal of Chemical Physics 1966;44:310–5.
[54] Fahrenfort J. Attenuated total reflection — a new principle for the production of useful infra-red reflection spectra of organic compounds. Spectrochim Acta 1961;17:698–709.
[55] Binder H. The molecular architecture of lipid membranes — new insights from hydration-tuning infrared linear dichroism spectroscopy. Appl Spectrosc Rev 2003;38:15–69.
[56] Goormaghtigh E, Raussens V, Ruysschaert JM. Attenuated total reflection infrared spectroscopy of proteins and lipids in biological membranes. Biochim Biophys Acta Rev Biomembr 1999;1422:105–85.
[57] Dluhy RA, Cornell DG. In situ measurement of the infrared-spectra of insoluble monolayers at the air–water-interface. J Phys Chem 1985;89:3195–7.
[58] Mendelsohn R, Brauner JW, Gericke A. External infrared reflection–absorption spectrometry monolayer films at the air–water-interface. Annu Rev Phys Chem 1995;46:305–34.
[59] Golden WG, Dunn DS, Overend J. A method for measuring infrared reflection–absorption spectra of molecules adsorbed on low-area surfaces at monolayer and submonolayer concentrations. J Catal 1981;71:395–404.
[60] Blaudez D, Buffeteau T, Cornut JC, Desbat B, Escafre N, Pezolet M, et al. Polarization-modulated FT-IR spectroscopy of a spread monolayer at the air–water-interface. Appl Spectrosc 1993;47:869–74.
[61] Blaudez D, Buffeteau T, Cornut JC, Desbat B, Escafre N, Pezolet M, et al. Polarization modulation ftir spectroscopy at the air–water-interface. Thin Solid Films 1994;242:146–50.
[62] Ataka K, Heberle J. Biochemical applications of surface-enhanced infrared absorption spectroscopy. Anal Bioanal Chem 2007;388:47–54.
[63] Osawa M. Surface-enhanced infrared absorption. Near-field Opt Surf Plasmon Polaritons 2001;81:163–87.
[64] Mendelsohn R, Flach CR. Handbook of vibrational spectroscopy. New Jersey: John Wiley & Sons; 2001.
[65] Mendelsohn R, Mao G, Flach CR. Infrared reflection–absorption spectroscopy: principles and applications to lipid–protein interaction in Langmuir films. Biochim Biophys Acta Biomembr 2010;1798:788–800.
[66] Shen YR. The principles of nonlinear optics. San Diego Academic Press; 1988 [Chapter 25].
[67] Shen YR. Surfaces probed by nonlinear optics. Surf Sci 1994;299:551–62.
[68] Boyd RW. Nonlinear optics. San Diego: Academic Press; 1992 439.
[69] Lambert AG, Davies PB, Neivandt DJ. Implementing the theory of sum frequency generation vibrational spectroscopy: a tutorial review. Appl Spectrosc Rev 2005;40:103–45.
[70] Williams CT, Beattie DA. Probing buried interfaces with non-linear optical spectroscopy. Surf Sci 2002;500:545–76.
[71] Shen YR. Phase-sensitive sum-frequency spectroscopy. In: Johnson MA, Martinez TJ, editors. Annual review of physical chemistry, vol. 64; 2013. p. 129–50.
[72] Geiger FM. Second harmonic generation, sum frequency generation, and chi((3)): dissecting environmental interfaces with a nonlinear optical Swiss army knife. Annu Rev Phys Chem 2009;60:61–83.
[73] Jubb AM, Hua W, Allen HC. Environmental chemistry at vapor/water interfaces: insights from vibrational sum frequency generation spectroscopy. In: Johnson MA, Martinez TJ, editors. Annual review of physical chemistry, vol. 63; 2012. p. 107–30.
[74] Raschke MB, Hayashi M, Lin SH, Shen YR. Doubly-resonant sum-frequency generation spectroscopy for surface studies. Chem Phys Lett 2002;359:367–72.
[75] Zhuang X, Miranda PB, Kim D, Shen YR. Mapping molecular orientation and conformation at interfaces by surface nonlinear optics. Phys Rev B 1999;59:12632–40.
[76] Guyot-Sionnest P, Hunt JH, Shen YR. Sum-frequency vibrational spectroscopy of a Langmuir film: study of molecular orientation of a two-dimensional system. Phys Rev Lett 1987;59:1597–600.
[77] Pavinatto FJ, Pacholatti CP, Montanha EA, Caseli L, Silva HS, Miranda PB, et al. Cholesterol mediates chitosan activity on phospholipid monolayers and Langmuir–Blodgett films. Langmuir 2009;25:10051–61.
[78] Miranda PB, Pflumio V, Saijo H, Shen YR. Surfactant monolayers at solid–liquid interfaces: conformation and interaction. Thin Solid Films 1998;327:161–5.
[79] Du Q, Freysz E, Shen YR. Vibrational-spectra of water-molecules at quartz water interfaces. Phys Rev Lett 1994;72:238–41.
[80] Belkin MA, Kulakov TA, Ernst KH, Yan L, Shen YR. Sum-frequency vibrational spectroscopy on chiral liquids: a novel technique to probe molecular chirality. Phys Rev Lett 2000;85:4474–7.
[81] Aroca R. Surface-enhanced vibrational spectroscopy. Chichester: John Wiley & Sons Ltd; 2006.
[82] Ru ECL, Etchegoin PG. Principles of surface-enhanced ramanspectroscopy: and related plasmonic effects. Oxford: Elsevier; 2008.
[83] Alessio P, Constantino CJL, Aroca RF, Oliveira Jr ON. Surface-enhanced Raman scattering: metal nanostructures coated with Langmuir–Blodgett films. J Chil Chem Soc 2010;55:469–78.
[84] Nikoobakht B, El-Sayed MA. Preparation and growth mechanism of gold nanorods (NRs) using seed-mediated growth method. Chem Mater 2003;15:1957–62.
[85] Rai A, Singh A, Ahmad A, Sastry M. Role of halide ions and temperature on the morphology of biologically synthesized gold nanotriangles. Langmuir 2006;22:736–41.
[86] Im SH, Lee YT, Wiley B, Xia YN. Large-scale synthesis of silver nanocubes: the role of HCl in promoting cube perfection and monodispersity. Angew Chem Int Ed 2005;44:2154–7.
[87] Li JF, Huang YF, Ding Y, Yang ZL, Li SB, Zhou XS, et al. Shell-isolated nanoparticle-enhanced Raman spectroscopy. Nature 2010;464:392–5.
[88] Guerrero AR, Aroca RF. Surface-enhanced fluorescence with shell-isolated nanoparticles (SHINEF). Angew Chem Int Ed 2011;50:665–8.
[89] Kneipp K, Haka AS, Kneipp H, Badizadegan K, Yoshizawa N, Boone C, et al. Surface-enhanced Raman spectroscopy in single living cells using gold nanoparticles. Appl Spectrosc 2002;56:150–4.
[90] Stender AS, Marchuk K, Liu C, Sander S, Meyer MW, Smith EA, et al. Single cell optical imaging and spectroscopy. Chem Rev 2013;113:2469–527.
[91] Tu RS, Tirrell M. Bottom-up design of biomimetic assemblies. Adv Drug Deliv Rev 2004;56:1537–63.
[92] Jones, Chapman. Micelles, monolayers and biomembranes. New York: Wiley-Liss; 1994.
[93] Brezesinski G, Mohwald H. Langmuir monolayers to study interactions at model membrane surfaces. Adv Colloid Interface Sci 2003;100:563–84.
[94] Gribova V, Auzely-Velty R, Picart C. Polyelectrolyte multilayer assemblies on materials surfaces: from cell adhesion to tissue engineering. Chem Mater 2012;24:854–69.
[95] Schmidt RC, Healy KE. Controlling biological interfaces on the nanometer length scale. J Biomed Mater Res A 2009;90A:1252–61.
[96] Holmes HN. A practical model of the animal cell membranes. J Phys Chem 1939;43:1151–3.
[97] Ross S. Solubilization of dyes in mineral oil and its application to a model biological cell membrane. J Colloid Sci 1951;6:497–507.
[98] Schreier S, Malheiros SVP, de Paula E. Surface active drugs: self-association and interaction with membranes and surfactants. Physicochemical and biological aspects. Biochim Biophys Acta Biomembr 2000;1508:210–34.
[99] Fa N, Ronkart S, Schanck A, Deleu M, Gaigneaux A, Goonnaghtigh E, et al. Effect of the antibiotic azithromycin on thermotropic behavior of DOPC or DPPC bilayers. Chem Phys Lipids 2006;144:108–16.
[100] Cancino J, Nobre TM, Oliveira Jr ON, Machado SAS, Zucolotto V. A new strategy to investigate the toxicity of nanomaterials using Langmuir monolayers as membrane models. Nanotoxicology 2013;7:61–70.
[101] Nguyen KT, Soong R, Im S-C, Waskell L, Ramamoorthy A, Chen Z. Probing the spontaneous membrane insertion of a tail-anchored membrane protein by sum frequency generation spectroscopy. J Am Chem Soc 2010;132:15112–5.
[102] Shen YR, Ostroverkhov V. Sum-frequency vibrational spectroscopy on water interfaces: polar orientation of water molecules at interfaces. Chem Rev 2006;106:1140–54.
[103] Ma G, Allen HC. DPPC Langmuir monolayer at the air–water interface: probing the tail and head groups by vibrational sum frequency generation spectroscopy. Langmuir 2006;22:5341–9.
[104] Sarangi NK, Patnaik A. Unraveling tryptophan modulated 2D DPPC lattices: an approach toward stimuli responsiveness of the pulmonary surfactant. J Phys Chem B 2011;115:13551–62.
[105] Diederich A, Sponer C, Pum D, Sleytr UB, Losche M. Reciprocal influence between the protein and lipid components of a lipid–protein membrane model. Colloids Surf B Biointerfaces 1996;6:335–46.
[106] Polverini E, Arisi S, Cavatorta P, Berzina T, Cristofolini L, Fasano A, et al. Interaction of myelin basic protein with phospholipid monolayers: mechanism of protein penetration. Langmuir 2003;19:872–7.
[107] Meister A, Nicolini C, Waldmann H, Kuhlmann J, Kerth A, Winter R, et al. Insertion of lipidated Ras proteins into lipid monolayers studied by infrared reflection absorption spectroscopy (IRRAS). Biophys J 2006;91:1388–401.
[108] Banc A, Desbat B, Renard D, Popineau Y, Mangavel C, Navailles L. Exploring the interactions of gliadins with model membranes: effect of confined geometry and interfaces. Biopolymers 2009;91:610–22.
[109] vandenAkker CC, Engel MFM, Velikov KP, Bonn M, Koenderink GH. Morphology and persistence length of amyloid fibrils are correlated to peptide molecular structure. J Am Chem Soc 2011;133:18030–3.
[110] Lopes DHJ, Meister A, Gohlke A, Hauser A, Blume A, Winter R. Mechanism of islet amyloid polypeptide fibrillation at lipid interfaces studied by infrared reflection absorption spectroscopy. Biophys J 2007;93:3132–41.
[111] Damalio JCP, Nobre TM, Lopes JL, Oliveira Jr ON, Araujo APU. Lipid interaction triggering Septin2 to assembly into beta-sheet structures investigated by Langmuir monolayers and PM-IRRAS. Biochim Biophys Acta Bioenerg 1828;2013:1441–8.
[112] Kong M, Chen XG, Xing K, Park HJ. Antimicrobial properties of chitosan and mode of action: a state of the art review. Int J Food Microbiol 2010;144:51–63.
[113] Mhurchu CN, Dunshea-Mooij C, Bennett D, Rodgers A. Effect of chitosan on weight loss in overweight and obese individuals: a systematic review of randomized controlled trials. Obes Rev 2005;6:35–42.

[114] Casal E, Montilla A, Moreno FJ, Olano A, Corzo N. Use of chitosan for selective removal of beta-lactoglobulin from whey. J Dairy Sci 2006;89:1384–9.
[115] Caseli L, Pavinatto FJ, Nobre TM, Zaniquelli MED, Viitala T, Oliveira Jr ON. Chitosan as a removing agent of beta-lactoglobulin from membrane models. Langmuir 2008;24:4150–6.
[116] Silva CA, Nobre TM, Pavinatto FJ, Oliveira Jr ON. Interaction of chitosan and mucin in a biomembrane model environment. J Colloid Interface Sci 2012;376:289–95.
[117] Finegold L. Cholesterol in membrane models. Boca Raton: CRC Press; 1993.
[118] Ohe C, Sasaki T, Noi M, Goto Y, Itoh K. Sum frequency generation spectroscopic study of the condensation effect of cholesterol on a lipid monolayer. Anal Bioanal Chem 2007;388:73–9.
[119] Pott T, Maillet JC, Dufourc EJ. Effects of pH and cholesterol on DMPA membranes: a solid state H-2- and P-31-NMR study. Biophys J 1995;69:1897–908.
[120] Chieze L, Bolanos-Garcia VM, Pinot M, Desbat B, Renault A, Beaufils S, et al. Fluid and condensed ApoA-I/phospholipid monolayers provide insights into ApoA-I membrane insertion. J Mol Biol 2011;410:60–76.
[121] Nobre TM, de Sousa e Silva H, Furriel RPM, Leone FA, Miranda PB, Zaniquelli MED. Molecular view of the interaction between iota-carrageenan and a phospholipid film and its role in enzyme immobilization. J Phys Chem B 2009;113:7491–7.
[122] Chen X, Wang J, Boughton AP, Kristalyn CB, Chen Z. Multiple orientation of melittin inside a single lipid bilayer determined by combined vibrational spectroscopic studies. J Am Chem Soc 2007;129:1420–7.
[123] Chen X, Wang J, Kristalyn CB, Chen Z. Real-time structural investigation of a lipid bilayer during its interaction with melittin using sum frequency generation vibrational spectroscopy. Biophys J 2007;93:866–75.
[124] Xiao D, Fu L, Liu J, Batista VS, Yan ECY. Amphiphilic adsorption of human islet amyloid polypeptide aggregates to lipid/aqueous interfaces. J Mol Biol 2012;421:537–47.
[125] Kouzayha A, Nasir MN, Buchet R, Wattraint O, Sarazin C, Besson F. Conformational and interfacial analyses of K(3)A(18)K(3) and alamethicin in model membranes. J Phys Chem B 2009;113:7012–9.
[126] Wieclaw K, Korchowiec B, Corvis Y, Korchowiec J, Guermouche H, Rogalska E. Meloxicam and meloxicam–beta–cyclodextrin complex in model membranes: effects on the properties and enzymatic lipolysis of phospholipid monolayers in relation to anti-inflammatory activity. Langmuir 2009;25:1417–26.
[127] Pinheiro M, Lucio M, Reis S, Lima JLFC, Caio JM, Moiteiro C, et al. Molecular interaction of rifabutin on model lung surfactant monolayers. J Phys Chem B 2012;116:11635–45.
[128] Flach CR, Gericke A, Keough KMW, Mendelsohn R. Palmitoylation of lung surfactant protein SP-C alters surface thermodynamics, but not protein secondary structure or orientation in 1,2-dipalmitoylphosphatidylcholine Langmuir films. Biochim Biophys Acta Biomembr 1999;1416:11–20.
[129] Dieudonne D, Mendelsohn R, Farid RS, Flach CR. Secondary structure in lung surfactant SP-B peptides: IR and CD studies of bulk and monolayer phases. Biochim Biophys Acta Biomembr 2001;1511:99–112.
[130] Stenger PC, Alonso C, Zasadzinski JA, Waring AJ, Jung C-L, Pinkerton KE. Environmental tobacco smoke effects on lung surfactant film organization. Biochim Biophys Acta Biomembr 2009;1788:358–70.
[131] Pavinatto FJ, Caseli L, Pavinatto A, dos Santos Jr DS, Nobre TM, Zaniquelli MED, et al. Probing chitosan and phospholipid interactions using Langmuir and Langmuir–Blodgett films as cell membrane models. Langmuir 2007;23:7666–71.
[132] Caseli L, Zaniquelli MED, Furriel RPM, Leone FA. Enzymatic activity of alkaline phosphatase adsorbed on dimyristoylphosphatidic acid Langmuir–Blodgett films. Colloids Surf B Biointerfaces 2002;25:119–28.
[133] Schmidt TF, Pavinatto FJ, Caseli L, Gonzaga MLC, Soares SA, Ricardo NMPS, et al. Interaction of polysaccharide–protein complex from *Agaricus blazei* with Langmuir and Langmuir–Blodgett films of phospholipids. J Colloid Interface Sci 2009;330:84–9.
[134] Schmidt TF, Caseli L, Viitala T, Oliveira Jr ON. Enhanced activity of horseradish peroxidase in Langmuir–Blodgett films of phospholipids. Biochim Biophys Acta Biomembr 2008;1778:2291–7.
[135] Wang T, Li D, Lu X, Khmaladze A, Han X, Ye S, et al. Single lipid bilayers constructed on polymer cushion studied by sum frequency generation vibrational spectroscopy. J Phys Chem C 2011;115:7613–20.
[136] Ye S, Li H, Wei F, Jasensky J, Boughton AP, Yang P, et al. Observing a model ion channel gating action in model cell membranes in real time in situ: membrane potential change induced alamethicin orientation change. J Am Chem Soc 2012;134:6237–43.
[137] Laredo T, Dutcher JR, Lipkowski J. Electric field driven changes of a gramicidin containing lipid bilayer supported on a Au(111) surface. Langmuir 2011;27:10072–87.
[138] Leitch JJ, Brosseau CL, Roscoe SG, Bessonov K, Dutcher JR, Lipkowski J. Electrochemical and PM-IRRAS characterization of cholera toxin binding at a model biological membrane. Langmuir 2013;29:965–76.
[139] Pilbat A-M, Szegletes Z, Kota Z, Ball V, Schaaf P, Voegel J-C, et al. Phospholipid bilayers as biomembrane-like barriers in layer-by-layer polyelectrolyte films. Langmuir 2007;23:8236–42.
[140] Henry ER, Hofrichter J. Singular value decomposition — application to analysis of experimental-data. Methods Enzymol 1992;210:129–92.
[141] Barraud A, Perrot H, Billard V, Martelet C, Therasse J. Study of immunoglobulin-g thin-layers obtained by the Langmuir–Blodgett method — application to immunosensors. Biosens Bioelectron 1993;8:39–48.
[142] Singhal R, Gambhir A, Pandey MK, Annapoorni S, Malhotra BD. Immobilization of urease on poly(N-vinyl carbazole)/stearic acid Langmuir–Blodgett films for application to urea biosensor. Biosens Bioelectron 2002;17:697–703.
[143] Vinu A, Miyahara M, Ariga K. Biomaterial immobilization in nanoporous carbon molecular sieves: influence of solution pH, pore volume, and pore diameter. J Phys Chem B 2005;109:6436–41.
[144] Caseli L, Perinotto AC, Viitala T, Zucolotto V, Oliveira Jr ON. Immobilization of alcohol dehydrogenase in phospholipid Langmuir–Blodgett films to detect ethanol. Langmuir 2009;25:3057–61.
[145] Ohnuki H, Honjo R, Endo H, Imakubo T, Izumi M. Amperometric cholesterol biosensors based on hybrid organic–inorganic Langmuir–Blodgett films. Thin Solid Films 2009;518:596–9.
[146] Ohnuki H, Saiki T, Kusakari A, Endo H, Ichihara M, Izumi M. Incorporation of glucose oxidase into Langmuir–Blodgett films based on Prussian blue applied to amperometric glucose biosensor. Langmuir 2007;23:4675–81.
[147] Pakalns T, Haverstick KL, Fields GB, McCarthy JB, Mooradian DL, Tirrell M. Cellular recognition of synthetic peptide amphiphiles in self-assembled monolayer films. Biomaterials 1999;20:2265–79.
[148] Khopade AJ, Caruso F. Surface-modification of polyelectrolyte multilayer-coated particles for biological applications. Langmuir 2003;19:6219–25.
[149] Yang P, Zhang XX, Yang B, Zhao HC, Chen JC, Yang WT. Facile preparation of a patterned, aminated polymer surface by UV-light-induced surface aminolysis. Adv Funct Mater 2005;15:1415–25.
[150] Kennedy LJ, Selvi PK, Padmanabhan A, Hema KN, Sekaran G. Immobilization of polyphenol oxidase onto mesoporous activated carbons — isotherm and kinetic studies. Chemosphere 2007;69:262–70.
[151] Lu Z, Zhang J, Ma Y, Song S, Gu W. Biomimetic mineralization of calcium carbonate/carboxymethylcellulose microspheres for lysozyme immobilization. Mater Sci Eng C-Mater Biol Appl 2012;32:1982–7.
[152] Nicolau E, Mendez J, Fonseca JJ, Griebenow K, Cabrera CR. Bioelectrochemistry of non-covalent immobilized alcohol dehydrogenase on oxidized diamond nanoparticles. Bioelectrochemistry 2012;85:1–6.
[153] Sun J, Ma H, Liu Y, Su Y, Xia W, Yang Y. Improved preparation of immobilized trypsin on superparamagnetic nanoparticles decorated with metal ions. Colloids Surf A Physicochem Eng Asp 2012;414:190–7.
[154] Matsuno H, Nagasaka Y, Kurita K, Serizawa T. Superior activities of enzymes physically immobilized on structurally regular poly(methyl methacrylate) surfaces. Chem Mater 2007;19:2174–9.
[155] Choi J, Konno T, Matsuno R, Takai M, Ishihara K. Surface immobilization of biocompatible phospholipid polymer multilayered hydrogel on titanium alloy. Colloids Surf B Biointerfaces 2008;67:216–23.
[156] Potara M, Gabudean AM, Astilean S. Solution-phase, dual LSPR–SERS plasmonic sensors of high sensitivity and stability based on chitosan-coated anisotropic silver nanoparticles. J Mater Chem 2011;21:3625–33.
[157] Ip S, MacLaughlin CM, Gunari N, Walker GC. Phospholipid membrane encapsulation of nanoparticles for surface-enhanced raman scattering. Langmuir 2011;27:7024–33.
[158] Kumar M, Muzzarelli RAA, Muzzarelli C, Sashiwa H, Domb AJ. Chitosan chemistry and pharmaceutical perspectives. Chem Rev 2004;104:6017–84.
[159] Hodges MD, Kelly JG, Bentley AJ, Fogarty S, Patel II, Martin FL, et al. Combining immunolabeling and surface-enhanced Raman spectroscopy on cell membranes. ACS Nano 2011;5:9535–41.
[160] Lee S, Chon H, Yoon SY, Lee EK, Chang SI, Lim DW, et al. Fabrication of SERS-fluorescence dual modal nanoprobes and application to multiplex cancer cell imaging. Nanoscale 2012;4:124–9.
[161] Pallaoro A, Braun GB, Reich NO, Moskovits M. Mapping local pH in live cells using encapsulated fluorescent SERS nanotags. Small 2010;6:618–22.
[162] Kennedy DC, Hoop KA, Tay LL, Pezacki JP. Development of nanoparticle probes for multiplex SERS imaging of cell surface proteins. Nanoscale 2010;2:1413–6.
[163] Zong SF, Wang ZY, Zhang RH, Wang CL, Xu SH, Cui YP. A multiplex and straightforward aqueous phase immunoassay protocol through the combination of SERS-fluorescence dual mode nanoprobes and magnetic nanobeads. Biosens Bioelectron 2013;41:745–51.
[164] Jiang L, Qian J, Cai FH, He SL. Raman reporter-coated gold nanorods and their applications in multimodal optical imaging of cancer cells. Anal Bioanal Chem 2011;400:2793–800.
[165] Syamala KM, Abe H, Fujita Y, Tomimoto K, Biju V, Ishikawa M, et al. Inhibition assay of yeast cell walls by plasmon resonance Rayleigh scattering and surface-enhanced Raman scattering imaging. Langmuir 2012;28:8952–8.
[166] Aoki PHB, Volpati D, Riul Jr A, Caetano W, Constantino CJL. Layer-by-layer technique as a new approach to produce nanostructured films containing phospholipids as transducers in sensing applications. Langmuir 2009;25:2331–8.
[167] Aoki PHB, Alessio P, Rodriguez-Mendez ML, De Saja Saez JA, Constantino CJL. Taking advantage of electrostatic interactions to grow Langmuir–Blodgett films containing multilayers of the phospholipid dipalmitoylphosphatidylglycerol. Langmuir 2009;25:13062–70.
[168] Moraes ML, Baptista MS, Itri R, Zucolotto V, Oliveira Jr ON. Immobilization of liposomes in nanostructured layer-by-layer films containing dendrimers. Mater Sci Eng C Biomim Supramol Syst 2008;28:467–71.
[169] Palyvoda O, Bordenyuk AN, Yatawara AK, McCullen E, Chen C-C, Benderskii AV, et al. Molecular organization in SAMs used for neuronal cell growth. Langmuir 2008;24:4097–106.
[170] Ye S, Nguyen KT, Boughton AP, Mello CM, Chen Z. Orientation difference of chemically immobilized and physically adsorbed biological molecules on polymers detected at the solid/liquid interfaces in situ. Langmuir 2010;26:6471–7.
[171] Miao S, Leeman H, De Feyter S, Schoonheydt RA. Facile preparation of Langmuir–Blodgett films of water-soluble proteins and hybrid protein-clay films. J Mater Chem 2010;20:698–705.

[172] Caseli L, Tiburcio VLB, Vargas FFR, Marangoni S, Siqueira Jr JR. Enhanced architecture of lipid-carbon nanotubes as Langmuir–Blodgett films to investigate the enzyme activity of phospholipases from snake venom. J Phys Chem B 2012; 116:13424–9.
[173] Nowak C, Laredo T, Gebert J, Lipkowski J, Gennis RB, Ferguson-Miller S, et al. 2D-SEIRA spectroscopy to highlight conformational changes of the cytochrome c oxidase induced by direct electron transfer. Metallomics 2011;3:619–27.
[174] Fan M, Marechal M, Finn A, Harrington DA, Brolo AG. Layer-by-layer characterization of a model biofuel cell anode by (in situ) vibrational spectroscopy. J Phys Chem C 2011;115:310–6.
[175] Snyder RG, Strauss HL, Elliger CA. C – H stretching modes and the structure of normal-alkyl chains.1. Long, disordered chains. J Phys Chem 1982;86:5145–50.
[176] Zhao L, Feng S-S. Effects of cholesterol component on molecular interactions between paclitaxel and phospholipid within the lipid monolayer at the air–water interface. J Colloid Interface Sci 2006;300:314–26.
[177] Florsheimer M, Brillert C, Fuchs H. Chemical imaging of interfaces by sum-frequency generation. Mater Sci Eng C Biomim Supramol Syst 1999;8–9:335–41.
[178] Cimatu K, Baldelli S. Sum frequency generation microscopy of microcontact-printed mixed self-assembled monolayers. J Phys Chem B 2006;110:1807–13.
[179] Schaller RD, Johnson JC, Wilson KR, Lee LF, Haber LH, Saykally RJ. Nonlinear chemical imaging nanomicroscopy: from second and third harmonic generation to multiplex (broad-bandwidth) sum frequency generation near-field scanning optical microscopy. J Phys Chem B 2002;106:5143–54.
[180] Huh YS, Chung AJ, Erickson D. Surface enhanced Raman spectroscopy and its application to molecular and cellular analysis. Microfluid Nanofluid 2009;6:285–97.
[181] Morita A, Ishiyama T. Recent progress in theoretical analysis of vibrational sum frequency generation spectroscopy. Phys Chem Chem Phys 2008;10:5801–16.
[182] Roke S, Gonella G. Nonlinear light scattering and spectroscopy of particles and droplets in liquids. In: Johnson MA, Martinez TJ, editors. Annual review of physical chemistry, vol. 63; 2012. p. 353–78.
[183] Kolano C, Helbing J, Kozinski M, Sander W, Hamm P. Watching hydrogen-bond dynamics in a beta-turn by transient two-dimensional infrared spectroscopy. Nature 2006;444:469–72.
[184] Li JJ, Yip CM. Super-resolved FT-IR spectroscopy: strategies, challenges, and opportunities for membrane biophysics. Biochim Biophys Acta Biomembr 1828;2013:2272–82.
[185] Aoki PHB, Carreon EGE, Volpati D, Shimabukuro MH, Constantino CJL, Aroca RF, et al. SERS mapping in Langmuir–Blodgett films and single-molecule detection. Appl Spectrosc 2013;67:563–9.